

1 **When local means local: Polygenic signatures of local adaptation within**
2 **whitebark pine (*Pinus albicaulis* Engelm.) across the Lake Tahoe Basin, USA**

3

4 Brandon M. Lind^{*1}, Christopher J. Friedline[†], Jill L. Wegrzyn[‡], Patricia E. Maloney[§], Detlev R.
5 Vogler^{**}, David B. Neale^{††}, and Andrew J. Eckert^{†2}

6

7 ^{*}Integrative Life Sciences program, Virginia Commonwealth University, Richmond, Virginia
8 23284 USA

9 [†]Department of Biology, Virginia Commonwealth University, Richmond, Virginia 23284 USA

10 [‡]Department of Ecology and Evolutionary Biology, University of Connecticut, Storrs, CT 06269
11 USA


12 [§]Department of Plant Pathology and Tahoe Environmental Research Center, University of
13 California, Davis, California 95616 USA

14 ^{**}USDA, Forest Service, Pacific Southwest Research Station, Institute of Forest Genetics, 2480
15 Carson Road, Placerville, California 95667 USA

16 ^{††}Department of Plant Sciences, University of California, Davis California 95616 USA

17

18 Data reference numbers (XXXXXXXXXXXX)

¹ Corresponding Author. Current Address: Integrative Life Sciences PhD. program, Virginia Commonwealth University, Richmond, VA 23284. E-mail: lindb@vcu.edu @iowensis

² Corresponding Author. Current Address: Department of Biology, Virginia Commonwealth University, Richmond, VA 23284. E-mail: aeckert2@vcu.edu

19 **Running Title:** Local adaptation of *P. albicaulis*

20

21 **Key words:**

22 Local adaptation, *Pinus albicaulis*, divergent selection, gene flow, linkage disequilibrium

23

24 Corresponding Authors:

25 Brandon M. Lind

26 1000 West Cary Street

27 Life Science Bldg. - Department of Biology Rm 126

28 Virginia Commonwealth University

29 Richmond, Virginia 23284 USA

30 e-mail: lindb@vcu.edu, fax: 804-828-0820

31

32 Andrew J. Eckert

33 1000 West Cary Street

34 Life Science Bldg. - Department of Biology Rm 126

35 Virginia Commonwealth University

36 Richmond, Virginia 23284 USA

37 e-mail: aeckert2@vcu.edu, fax: 804-828-0800

38

ABSTRACT

39

40

41

42

43

44

45

46

47

48

49

50

51

52

53

54

55

56

57

58

59

For populations exhibiting high levels of gene flow, the genetic architecture of fitness-related traits is expected to be polygenic and underlain by many small-effect loci that covary across a network of linked genomic regions. For most coniferous taxa, studies describing this architecture have been limited to single-locus approaches, possibly leaving the vast majority of the underlying genetic architecture undescribed. Even so, molecular investigations rarely search for patterns indicative of an underlying polygenic basis, despite prior expectations for this signal. Here, using a polygenic perspective, we employ single and multilocus analyses of genome-wide data ($n = 116,231$ SNPs) to describe the genetic architecture of adaptation within whitebark pine (*Pinus albicaulis* Engelm.) across the local extent of the environmentally heterogeneous Lake Tahoe Basin, USA. We show that despite highly shared genetic variation ($F_{ST} = 0.0069$) there is strong evidence for polygenic adaptation to the rain shadow experienced across the eastern Sierra Nevada. Specifically, we find little evidence for large-effect loci and that the frequencies of loci associated with 4/5 phenotypes (mean = 236 SNPs), 18 environmental variables (mean = 99 SNPs), and those detected through genetic differentiation ($n = 110$ SNPs) exhibit significantly higher covariance than random SNPs. We also provide evidence that this covariance tracks environmental measures related to soil water availability through subtle allele frequency shifts across populations. Our results provide replicative support for theoretical expectations and highlight advantages of a polygenic perspective, as unremarkable loci when viewed from a single-locus perspective are noteworthy when viewed through a polygenic lens, particularly when considering protective measures such as conservation guidelines and restoration strategies.

60

INTRODUCTION

61 Shortly after Nilsson-Ehle (1909) and East (1910) independently demonstrated evidence for
62 multiple-factor inheritance, Fisher (1918) laid the groundwork for quantitative genetics by
63 incorporating the additive properties of variance to partition phenotypic variation into
64 components tractable to a model of Mendelian inheritance. It was this work, and that of Fisher's
65 infinitesimal model (1930), which founded the basis for attributing continuous variation of
66 phenotypes to a polygenic model of many underlying heritable components of small effect.
67 There, Fisher (1930) characterized adaptation as the non-random advance of a population's
68 mean phenotype towards an optimum that best fits its environment. Correspondingly, when
69 selective forces are spatially heterogeneous, populations can become locally adapted. Indeed,
70 over the subsequent century since Fisher's insight, local adaptation has been demonstrated to
71 occur across numerous taxa. As such, the study of local adaptation has been an integral part of
72 evolutionary biology as a whole, as local adaptation influences a wide variety of biological
73 patterns and processes (reviewed in Savolainen *et al.* 2013; Tigano and Friesen 2016). Plants
74 in particular have received much attention in this regard due in part to ideal characteristics
75 within native populations and environments that lend themselves to such analyses. Through
76 these investigations, local adaptation in plants appears to be common, yet the genetic
77 architecture (i.e., the number, effect size, type, and interaction of loci) of local adaptation in
78 natural populations remains largely undescribed (Leimu and Fischer 2008; Hereford 2009).

79 Investigators seeking to explain the genetic basis of local adaptation in plants have been
80 motivated by observations of significant phenotypic differentiation among populations (e.g.,
81 Q_{ST}). If such phenotypes have a genetic basis, the underlying QTL may be differentiated among
82 populations as well (Endler 1977; reviewed in Storz 2005, Haasl and Payseur 2016). In such
83 cases, loci contributing to local adaptation could be identified through genetic indices of
84 differentiation, or by targeting trait- or environmentally-associated loci that stand out above
85 background demography. Yet, theoretical (Latta 2003; Le Corre and Kremer 2003) and

86 empirical (Hall *et al.* 2007; Luquez *et al.* 2007) investigations exploring the relationship between
87 phenotypic differentiation (e.g., Q_{ST}) and that of the underlying loci (e.g., G_{ST} or F_{ST}) have shown
88 that discordance between these two structural indices can occur under adaptive evolution.
89 Moreover, as the number of underlying loci increases, the divergence between these indices
90 increases as well, and the contribution of F_{ST} to any individual underlying locus decreases. In
91 cases that exhibit strong diversifying selection and high gene flow, this adaptive divergence
92 results from selection on segregating genetic variation (Hermisson and Pennings 2005; Barret
93 and Schluter 2008) and is attributable to the between-population component of linkage
94 disequilibrium (Ohta 1982, Latta 1998). In the short term, local adaptation will be realized
95 through subtle coordinated shifts of allele frequencies across populations causing covariance
96 (i.e., LD) among many loci (Latta 1998; Barton 1999; Latta 2003; McKay and Latta 2002;
97 Kremer and Le Corre 2012; Le Corre and Kremer 2012), such that adaptation need not take
98 place through numerous fixation events or sweeping allele frequency changes (MacKay *et al.*
99 2009; Pritchard and di Rienzo 2010). Over many generations these shifts can lead to
100 concentrated architectures of large-effect loci with a reduction of those with small effect
101 (Yeaman and Whitlock 2011). For studies investigating continuous phenotypes such as those
102 often related to fitness, even among populations with highly differentiated phenotypic traits
103 sampled under a robust design (Lotterhos and Whitlock 2015), it may be difficult to discern if the
104 focal loci offer a representative picture of the underlying genetic architecture. Thus for many
105 species, specifically across fine spatial scales, the signal of polygenic local adaptation within
106 much of current genetic data may go largely undetected using only single-locus approaches
107 (Latta 1998; 2003; Le Corre and Kremer 2003; Yeaman and Whitlock 2011; Kemper *et al.*
108 2014), resulting in calls for theory and empiricism that move beyond single-locus perspectives
109 (Pritchard and di Rienzo 2010; Sork *et al.* 2013; Tiffin and Ross-Ibarra 2014; Stephan 2015).

110 Populations of forest trees, particularly conifers, have a rich history of common garden,
111 provenance tests, and genealogical studies that demonstrate abundant evidence for local

112 adaptation among populations, even over short geographic distances (e.g., Mitton 1989; 1999;
113 Budde *et al.* 2014; Csilléry *et al.* 2014; Vizcaíno *et al.* 2014; Eckert *et al.* 2015) providing further
114 support that fine spatial scales are relevant to adaptation (Richardson *et al.* 2014). This
115 extensive history has also revealed the highly polygenic nature of adaptive traits (Langlet 1971;
116 Holland 2007). Even so, the majority of these investigations have been limited to single-locus
117 perspectives using either candidate genes (e.g., González-Martínez *et al.* 2008; Eckert *et al.*
118 2009) or a large set of molecular markers (e.g., Eckert *et al.* 2010) to explain the genetic basis
119 of local adaptation. In most cases, a few moderate- to large-effect loci underlying the adaptive
120 trait in question explain were identified (Neale and Savolainen 2004; Savolainen *et al.* 2007;
121 Čalić *et al.* 2016). Yet because of the presumed polygenic nature underlying these adaptive
122 phenotypic traits, and because past investigations have generally applied single-locus
123 perspectives, it is likely that a majority of the genetic architecture of local adaptation in trees
124 remains undescribed as well (Savolainen 2007; Sork *et al.* 2013; Čalić *et al.* 2016).

125 Spurred in part by the advance of theory and availability of genome-wide marker data,
126 attention has been refocused to describe underlying genetic architectures from a polygenic
127 perspective. This transition began in model organisms (e.g., Turchin *et al.* 2012) and has
128 expanded to other taxa such as stick insects (Comeault *et al.* 2014; 2015), salmon (Bourret *et*
129 *al.* 2014), and trees (Ma *et al.* 2010; Csilléry *et al.* 2014; Hornoy *et al.* 2015). Indeed, species
130 that occupy landscapes with high degrees of environmental heterogeneity offer exemplary
131 cases with which to investigate local adaptation. Near its southern range limit, whitebark pine
132 (*Pinus albicaulis* Engelm.) populations of the Lake Tahoe Basin (LTB) inhabit a diversity of
133 environmental conditions. As exemplified by the strong west to east precipitation gradient (see
134 Figure 1), many of the environmental characteristics of the LTB vary over short physical
135 distances (<1km) and have the potential to shape geographic distributions of *P. albicaulis* at
136 spatial scales below those typically investigated (i.e., range-wide studies) for forest trees. Local
137 spatial scales are of particular interest to resource and conservation agencies as this is the

138 scale at which most management is applied. Here, we build upon past work from a common
139 garden (Maloney *et al. in review*) to investigate the genetic architecture of fine-scale local
140 adaptation across *P. albicaulis* populations of the LTB by exploring the relationships between
141 genotype, 18 environmental variables, and five fitness-related phenotypic traits using both
142 single and multilocus approaches. Specifically, we address the following four questions: (i) What
143 is the number, effect size distribution, and relationship among SNPs associated with
144 environment or phenotype? (ii) To what degree is there overlap of the loci identified through
145 environmental association with those identified through phenotypic association? (iii) Do focal
146 loci show higher degrees of evidence for natural selection acting on a polygenic architecture
147 (covariance of allele frequencies) than random loci within the genome? (iv) Is the covariance of
148 allele frequencies across population pairs associated with environmental heterogeneity? This
149 study highlights the advantages of a polygenic perspective and investigates signatures of local
150 adaptation using a large set of null markers to judge the extremity of allele covariation among
151 putatively adaptive loci where others have relied on simulation or null candidate genes.
152 Furthermore, this work provides additional replication for the support of theoretical predictions
153 for the covariation among adaptive loci found by other studies in trees.

154 MATERIALS and METHODS

155 *Focal species, study area, and sampling*

156 A principal component of high elevation forests in California and Nevada, *P. albicaulis* is
157 widespread throughout subalpine and treeline environments and plays a vital role in ecosystem
158 function and services including food resources for wildlife, forest cover, watershed protection,
159 protracting snowmelt, and biodiversity (Hutchins and Lanner 1982; Farnes 1990; Tomback et
160 al., 2001; McKinney et al., 2009; Tomback and Achuff 2010; Tomback et al. 2016). Most of the
161 species' distribution is outside of California, extending northward into Oregon, Washington, Brit-
162 ish Columbia, and Alberta and eastward into northern Nevada, Idaho, Montana, and Wyoming
163 (Critchfield and Little 1966; Tomback and Achuff 2010). Whitebark pine is a foundation species

164 in subalpine ecosystems throughout most of its range in western North America (Ellison et al.
165 2005) and is threatened by fire-suppression, climate change, the non-native pathogen white
166 pine blister rust, caused by *Cronartium ribicola* J.C. Fisch., and mountain pine beetle,
167 *Dendroctonus ponderosae* Hopkins (Tomback and Achuff 2010; Mahalovich and Stritch 2013).

168 The LTB lies within California and Nevada in the north-central Sierra Nevada range, varies
169 in elevation from 1900 to 3300m, and is flanked to the west by the Sierra Nevada crest and to
170 the east by the Carson Range. The LTB experiences a Mediterranean climate with warm, dry
171 summers and cool, wet winters. Precipitation falls during the winter months, most often in the
172 form of snow, with a strong west-east gradient. The geology of the region is dominated by
173 igneous intrusive rocks, typically granodiorite, and igneous extrusive rocks, typically andesitic
174 lahar, with small amounts of metamorphic rock (USDA NRCS 2007).

175 Each of the eight study populations (three subplots per population) was located in a distinct
176 watershed and were distributed around the Basin to capture variation in the physical
177 environment (e.g., climate, geology, and topography; Figure 1). Needle tissue was sampled in
178 the summer of 2008 from 244 *P. albicaulis* trees (Table 1). From these eight populations, six
179 populations were chosen to sample cones from 88 of the trees that were sampled for needle
180 tissue. All samples were collected from trees separated by 30 to 1000m, with an average
181 interpopulation distance of 31km. Universal Transverse Mercator coordinates, elevation, slope,
182 and aspect (USDA FS FHTET) were used with the PRISM climatic model (Daly *et al.* 1994) to
183 determine climatic parameters of sampled areas from 1971-2000 while soil survey data (USDA
184 NRCS 2007) were used to describe the edaphic conditions of the LTB (Table 1).

185 *Common gardens and phenotypic measurements*

186 For populations of forest trees, fitness-related traits associated with survival, especially
187 during seedling and juvenile stages, are an important component of total lifetime fitness and are
188 likely to be composed of phenotypic traits related to growth, phenology, resource allocation
189 patterns, water-use efficiency, and disease susceptibility. In order to estimate early-lifetime

190 phenotypes of mother trees, seeds sampled from 11 to 19 maternal trees ($n = 88$) located in six
191 of the eight populations were established in a common garden (Table 1) using a random block
192 design (for further details see Maloney *et al. in review*). Growth (height, root:shoot biomass),
193 phenology (budset), water-use efficiency ($\delta^{13}\text{C}$), and resource allocation ($\delta^{15}\text{N}$) were measured
194 when seedlings reached ~2 years in age (see Maloney *et al. in review* for details). Height was
195 recorded in April and October 2011, while 2 seedlings per family per block were harvested,
196 clipped above the root collar, dried, and weighed to determine root and shoot biomass. For $\delta^{13}\text{C}$
197 and $\delta^{15}\text{N}$ analysis, needle tissue from 1 seedling per family per block was harvested, coarsely
198 ground, and dried at 60°C for 96 hours. Between 2-3mg of tissue per sample was sent to the
199 Stable Isotope Facility at UC Davis for isotope analyses (<http://stableisotopefacility.ucdavis.edu/>).

200 Values for each phenotype were estimated for maternal trees (i.e. families) using linear
201 mixed models of the form:

$$202 \quad Y_{ijklm} = \mu + pop_i + fam(pop)_{j(i)} + block_k + date_l + \varepsilon_{ijklm},$$

203 where Y_{ijklm} is the phenotype of the m^{th} seedling sowed in the l^{th} year within the k^{th} block
204 originating from the j^{th} family nested within the i^{th} population, μ is the grand mean, pop_i is the
205 random effect of the i^{th} population, $fam(pop)_{j(i)}$ is the random effect of the j^{th} family nested within
206 the i^{th} population, $block_k$ is the fixed effect of the k^{th} block, $date_l$ is the effect of the l^{th} sowing
207 year, and ε_{ijklm} is the residual error of the m^{th} seedling sowed in the l^{th} year within the k^{th} block
208 originating from the j^{th} family nested within the i^{th} population. Separate models were fit to the
209 data for each phenotype using restricted maximum likelihood estimation (REML) as employed in
210 the `lme4` library (v1.1-12) in R (v3.2.2, R Core Team 2015). Effects of families were estimated
211 as the sum of the grand mean, the population effect, and the effect of family. Estimated values
212 were reported on the original scale of measurements of each phenotype, which were then used
213 in downstream analyses. In a previous study (Maloney *et al. in review*) we also estimated
214 narrow sense heritability and Q_{ST} (see Appendix).

215 **DNA extraction, sequencing, and analysis**

216 Total genomic DNA was isolated from finely ground needle tissue sampled from 244 trees
217 across all 8 populations using the Qiagen DNEasy 96 Plant kit according to protocol (Qiagen,
218 Germantown, MD), except that each sample was eluted twice with 50 μ L of the elution buffer to
219 increase DNA yield, as recommended by Qiagen. Restriction site-associated double digests of
220 total genomic DNA using MseI and EcoRI enzymes (ddRADSeq, Peterson *et al.* 2012) were
221 used to prepare three multiplexed libraries of up to 96 individuals each, as in Parchman *et al.*
222 (2012). For each library, one individual was duplicated in a separate well to increase coverage
223 for the downstream reference assembly. Total genomic DNA was digested and ligated with
224 adapters containing amplification and sequencing primers as well as barcodes for multiplexing.
225 These 96 barcodes (Parchman *et al.* 2012) are of 8-10bp sequences that differ by at least four
226 bases. Ligated DNA was then amplified using high-fidelity PCR according to manufacturer's
227 specifications. Using the QIAquick Gel Extraction Kit (Qiagen), amplified fragments were then
228 isolated near 400bp by excising the 300-500bp window of pooled PCR product separated in a
229 1% agarose gel at 100V for one hour. Single-end sequencing of libraries was carried out on the
230 Illumina HiSeq 2500 platform with a single library per flowcell lane. For added coverage, each
231 library was sequenced twice using 50bp reads and twice for 150bp reads, except Library 3
232 which was sequenced 4x for 150bp reads to increase optimality of the mapping reference
233 individual. All sequencing was performed at the DNA Sequencing Facility of the University of
234 California at Berkeley (<https://mcb.berkeley.edu/barker/dnaseq/home>).

235 Reads were assigned to individual sample IDs based on 100% match to the barcode
236 sequence or were otherwise discarded. The reads from the individual with the greatest number
237 of reads was assembled using Velvet (v1.2.1, Zerbino 2008) optimized for hash length k for
238 odd k on k ([37,49]) using VelvetOptimiser (v2.2.5, Gladman and Seemann 2016) where the
239 `-short` and `-short2` flags were used to distinguish the 150bp and 50bp reads, respectively.
240 To call SNPs for all individuals, reads were mapped to the reference assembly using Bowtie2

241 (v2.2.6, `--local -D 20 -R 3 -N 1 -L 20 -i S, 1, 0.50`; Langmead and Salzberg 2012).
242 samtools (v1.3, Li *et al.* 2009) was used to convert the resulting .sam files into their binary
243 (.bam) equivalent (`view, sort, index`). Genotypes were then called using bcftools (v1.3)
244 based on likelihoods estimated by samtools in mpileup. Genotypes were filtered with
245 vcftools (v0.1.13, Danecek *et al.* 2011) to enforce diallelic loci, remove indels and minor
246 allele frequency (MAF) of ≤ 0.01 , and exclude sites with $>50\%$ missing data.

247 Two datasets were created each starting with the same set of SNPs remaining after filtering.
248 The first dataset was left as-is to leave missing data (missing dataset, hereafter MDS). The
249 second dataset was created in which the missing data were imputed (imputed dataset, hereafter
250 IDS) using Beagle (v4.0, Browning and Browning 2016). Next, each of these two datasets was
251 analyzed using custom Python (v2.7.11) scripts to filter SNPs by removing those with minor
252 allele frequency <0.01 and global outliers for Wright's fixation index ($F > 0.5$ and $F < -0.5$). To
253 remove low coverage and artifacts of amplification, SNPs were removed if read depth was $<$
254 100 or ≥ 1500 . Each dataset was then reduced further to include only the intersection of loci
255 remaining between the two sets. To reduce physical linkage within our data, one SNP per contig
256 from the MDS was chosen by the least missing data. These SNPs were used to define a subset
257 from the IDS as the final empirical set of SNPs used for downstream analyses. To judge
258 veracity of sequence data we mapped the empirical set of SNPs against the sugar pine (*P.*
259 *lambertiana* Dougl.) reference genome (v1.0) using 85% similarity and 50% length coverage
260 thresholds (http://dendrome.ucdavis.edu/ftp/Genome_Data/genome/pinerefseq/Pila/v1.0/).

261 *Identifying loci under selection*

262 Linear mixed models (LMM) and sparse regression models, such as Bayesian variable
263 selection regression (BVSR, e.g., Guan and Stephens 2011) have been used to uncover
264 adaptive traits under a multilocus perspective. Yet the underlying assumptions of these models
265 differ in meaningful ways, particularly for polygenic modeling. In the case of LMM, the number of
266 underlying loci which affect the phenotype is assumed to be large, effectively every variant, with

267 a normal distribution of effect sizes (Zhou *et al.* 2013). Conversely, BVSR assumes that the
268 number of variants affecting the phenotype is small and represented by a point-normal
269 distribution of effect sizes (i.e., the effects come from a mixture of a normal distribution and a
270 point mass at 0; Guan and Stephens 2011). In this way, the LMM effectively assumes a large
271 number of small effects while the BVSR assumes a small number of larger effects (Zhou *et al.*
272 2013). Model selection between such methods should therefore depend upon the underlying
273 genetic architecture, which is generally not known beforehand. Because the genetic architecture
274 of the traits investigated here is unknown, we implemented a Bayesian sparse linear mixed
275 model (BSLMM) from the GEMMA software package (Zhou *et al.* 2013). BSLMM is a hybrid of
276 LMM and BVSR that also offers considerable statistical advantages over single-locus GWAS
277 approaches (Guan and Stephens 2011; Ehret *et al.* 2012; Zhou *et al.* 2013; Moser *et al.* 2015).
278 BSLMM accounts for population structure and relatedness then subsequently identifies which
279 relevant genetic variants to include in a multiple regression of the phenotype. Specifically, to
280 describe the underlying genetic architecture, BSLMM uses priors (described below) and
281 attributes of the genetic data to estimate the number of SNPs underlying a given trait (N_{SNP}), the
282 posterior inclusion probability (γ , hereafter *PIP*) for individual SNPs, the random (α ; i.e.,
283 polygenic) effect of SNPs included in the model (in standard deviations), the fixed (β , i.e.,
284 sparse) effects of SNPs included in the model (in standard deviations), the total effect ($\alpha + \beta\gamma$;
285 i.e., the combined effects of small- and large-effect SNPs), as well as the proportion of
286 phenotypic variance explained by the fixed effects and random effects combined (*PVE*, i.e., by
287 the total effect estimated from SNPs included in the model).

288 Before input to GEMMA, the empirical set of SNPs was reduced to include only those
289 individuals with seedlings in the common garden ($n = 88$) and loci which had MAF below 0.01
290 due to this reduction were eliminated alongside monomorphic SNPs. To account for population
291 structure, principal component analyses (PCAs) were calculated using the centered and
292 standardized mean genotypes of each SNP (based on the global MAF, following Patterson *et al.*

293 2006) and the `prcomp()` function in R. Significant PCs ($\alpha = 0.05$) were identified using a Tracy-
294 Widom test and were then used in linear models predicting each previously-estimated
295 phenotypic value from the common garden (Maloney *et al. in review*) using the `lm()` function in
296 R (phenotype ~ PCs). From these linear models, the trait-specific residuals were quantile-
297 transformed and were used to create the phenotypic in-files to GEMMA (as recommended by
298 Guan and Stephens 2011; Zhou *et al.* 2013). For each phenotype, we ran four independent
299 chains for the BSLMM, with 1,000,000 warm-up steps and 50,000,000 steps in the MCMC
300 which were sampled every 1000th step. Priors for the proportion of variance explained by the
301 model, h , were set as [0.01,0.9], and the \log_{10} inverse number of SNPs, $\log_{10}(1/p)$, [-3.0,0.0],
302 which equates to between 1 and 300 underlying loci (N_{SNP}). Convergence of the MCMC across
303 chains was visually inspected using the `coda` library in R. To summarize the GEMMA output, we
304 report means and 95% credible intervals for PVE and N_{SNP} from the posterior distributions. To
305 assess significance of association of a SNP to a phenotype, we used the posterior inclusion
306 probability from all four independent chains to calculate the harmonic mean (\overline{PIP}) and chose
307 SNPs that were greater than or equal to the 99.9th percentile of \overline{PIP} ($n \approx 116$ SNPs) for each
308 phenotype. We also explored SNPs with $\overline{PIP} \geq 99.8^{\text{th}}$ percentile ($n \approx 232$). Finally, we calculated
309 harmonic mean across chains for fixed ($\bar{\beta}$), random ($\bar{\alpha}$), and total effects ($\hat{b} = \bar{\alpha} + \bar{\beta} \cdot \overline{PIP}$).

310 To identify genotype-environmental associations, we implemented `bayenv2` (v2.0; Coop *et*
311 *al.* 2010; Günther and Coop 2013), a Bayesian single-locus approach that accounts for
312 population history and gene flow before performing association analysis (Coop *et al.* 2010). To
313 ensure convergence, we ran five independent chains of `bayenv2` using the IDS SNPs ($n =$
314 116,231), with 100,000 iterations for each SNP within each chain. Convergence of the MCMC
315 across chains was visually inspected using the `coda` library in R. For each SNP, we took the
316 harmonic mean across chains for the Bayes factor (\overline{BF}) and absolute value of Spearman's ρ
317 (hereafter $\overline{\rho_S}$). When calculating \overline{BF} , we further checked for convergence by flagging SNPs

318 which had large differences between values across chains. If a particular SNP returned Bayes
319 factors greater than one for at least 3/5 chains, we would take the harmonic mean from this
320 subset to avoid underestimation of the Bayes factor. However, if this was not the case ($BF > 1$
321 in $\leq 2/5$ chains) we took the harmonic mean from the values that were less than or equal to one.
322 We identified SNPs as those most likely to be associated with environmental variables by the
323 intersection between the upper tail (99.5th percentile) of \overline{BF} and the upper tail (99th percentile) of
324 the absolute value of $\overline{\rho_S}$, as recommended in the `bayenv2` manual (v2.0; page 4).

325 We implemented the program `OutFLANK` (Whitlock and Lotterhos 2015) to investigate
326 the opportunity of detecting the environmentally- and phenotypically-associated loci using outlier
327 approaches based on population genetic structure alone (e.g., F_{ST}). While F_{ST} outlier
328 approaches do not take on a polygenic perspective *per se*, they do have the advantage of not
329 requiring the investigator to identify, *a priori*, the phenotypic and environmental variables most
330 important to local adaptation. `OutFLANK` is an approach which uses empirical data to infer the
331 null distribution of F_{ST} (F'_{ST}) for loci unlikely to be under spatially heterogeneous selection (upper
332 tail of F'_{ST}) or homogenous balancing selection (lower tail of F'_{ST}). From this null distribution, focal
333 loci can be identified from the empirical set which show signatures of additional evolutionary
334 processes, such as spatially heterogeneous selection, with a lower false discovery rate and
335 comparable power relative to other outlier methods (Whitlock and Lotterhos 2015). Using this
336 approach and excluding loci with expected heterozygosity values below 10% with subsequent
337 trimming of the lower and upper 5% of empirical F_{ST} values, we inferred a null distribution of F'_{ST}
338 and identified outlier loci with a false discovery rate of 5% from the empirical set of SNPs.

339 *Inferring signatures of local adaptation*

340 Because of the polygenic basis expected from fitness-related traits, we investigated the level
341 of covariance of allele frequencies among focal SNPs identified from `GEMMA`, `bayenv2`, and
342 `OutFLANK` analyses with estimates of covariance among random SNPs chosen from bins

343 based on expected heterozygosity (H_E). For instance, to calculate the covariance of allele
344 frequencies across populations between two SNPs, SNP_i and SNP_j , within a focal set of SNPs
345 associated with a particular phenotype in GEMMA, we used the global minor allele of each SNP,
346 q , according to the interpopulation component of linkage disequilibrium,

$$347 \quad \hat{D}_{a(ij)} = \sum_k \frac{n_k}{n} (q_{i,k} q_{j,k} - q_i q_j) \quad \text{Eq. (1)}$$

348 where n_k is the number of individuals in population k , n is the global population size, $q_{i,k}$ is the
349 allele frequency of the i^{th} SNP in population k , $q_{j,k}$ is the allele frequency of the j^{th} SNP in
350 population k , while q_i and q_j are the respective global allele frequencies of the i^{th} and j^{th} SNP
351 across $k = 6$ populations (Storz and Kelly 2008, their Equation 2; Ma *et al.* 2010, their Equation
352 3). In some populations q_k was the major allele because we chose the allele to use in
353 comparisons based on global minor allele frequency. Therefore, all calculations of $\hat{D}_{a(ij)}$ are
354 referenced to the global minor allele haplotype for a pair of SNPs.

355 To be able to discern if the level of covariance of allele frequencies among SNPs
356 identified by GEMMA (or another method; hereafter focal SNPs) was greater than that from SNPs
357 randomly chosen from our dataset, we first divided all SNPs in the dataset by their expected
358 heterozygosity into bins of 0.01 ranging from 0 to 0.50. For instance, a SNP with H_E of (0.000-
359 0.010] would be binned into the first bin, while an H_E of (0.490-0.500] would be binned into the
360 50th. We then created a set of SNPs from which to take randomized draws by subtracting the
361 focal SNPs from the full set of SNPs. Next, based on the number of focal SNPs, a random set of
362 SNPs equal in total size was selected, as well as in the same number of SNPs from a given
363 heterozygosity bin. We chose SNPs randomly in this way, 1000 times, each time calculating the
364 absolute value of $\hat{D}_{a(ij)}$ among SNP pairs within each set. From each of these 1000
365 distributions, we calculated 1000 median absolute $\hat{D}_{a(ij)}$ values to create a null distribution for
366 use in comparison to the median absolute \hat{D}_{ij} from the focal set of SNPs. If the median $\hat{D}_{a(ij)}$ is

367 greater among our focal SNPs than the 95th percentile of the null distribution of 1000 medians,
368 we will conclude that the focal SNPs identified by a given method are in higher degrees of
369 covariance than expected by chance. For populations that experience high levels of gene flow
370 and divergent phenotypic optima due to selection, $\widehat{D}_{a(ij)}$ is expected to be positive between
371 alleles of loci conferring a positive effect on the phenotype, negative between those alleles
372 among loci conferring opposite effect, and zero between (conditionally) neutrally loci (eq. [6] in
373 Latta 1998). Because we were not able to discern the direction of effect for alleles within each
374 population (as in e.g., Gompert *et al.* 2015), we chose to identify extreme values by taking the
375 absolute value of $\widehat{D}_{a(ij)}$ for each locus pair. We also calculated covariance for focal SNPs
376 associated with environmental variables from `bayenv2` and those identified as outliers from
377 `OutFLANK`. In these two cases we used allele frequencies across all eight populations.

378 To infer signatures of allele frequency shifts, we implemented an approach similar to
379 Equation 1 but instead of estimating $\widehat{D}_{a(ij)}$ across all populations we estimated $\widehat{D}_{a(ij)}$ across
380 populations in a pairwise fashion (hereafter $pw\widehat{D}_{a(ij)}$) using focal SNPs from a given method. In
381 this case, we calculated global allele frequency (q_i or q_j) based on the frequency of allele q
382 across the $k = 2$ populations (pop_l and pop_m) under consideration (where $n_l + n_m = n$). From
383 these estimates, we created a symmetric matrix of $pw\widehat{D}_{a(ij)}$ with columns and rows for
384 populations, and distances within the diagonal set to zero. To discern signals of allele frequency
385 shifts associated with environment, we implemented Mantel tests (Mantel 1967) using $pw\widehat{D}_{a(ij)}$
386 matrices against other population pairwise distance matrices such as geographic distance
387 inferred using great circle distances (km) following Vincenty's method, Euclidian distance
388 matrices for each of the five phenotypes and for each of the 18 environmental variables.
389 Because we chose to take absolute values of $pw\widehat{D}_{a(ij)}$ for each locus pair (as with $\widehat{D}_{a(ij)}$) we
390 note that the sign of the correlation coefficient, r , from Mantel tests may reflect the opposite
391 directionality for any given SNP pair. Mantel tests were run with 9999 iterations using the `skbio`

392 package (v0.4.2) in Python. Each environmental or phenotypic value was centered and
393 standardized across populations before calculating Euclidian distances, but not for $pw\hat{D}_{a(ij)}$ or
394 geographic distance matrices. For each set of focal SNPs associated with phenotype or
395 environment, we quantified the mean allele frequency differences across populations and
396 compared this to 1000 sets of random SNPs chosen by H_E . To investigate evidence for
397 associations between sampled locations among environmental variables or among phenotypes,
398 we ran additional Mantel tests for each comparison.

399 **Data availability**

400 Sequence data is deposited in the short read archive of the National Center for Bio-
401 technology Information (project number: TBD). Scripts used in analyses can be found in IPython
402 notebook format (Pérez and Granger 2007) at https://github.com/brandonlind/whitebark_pine.

403 **RESULTS**

404 **SNP filtering and characterization**

405 The sample chosen to make the reference assembly was that with the greatest number of
406 reads (N = 23,363,768), which was the individual duplicated in the third library. Optimization
407 with VelvetOptimiser ($k_{opt} = 45$) resulted in an assembly with 391,957 contigs (maximum
408 330bp per contig, 48,906,035 total bases across contigs). Using the reference assembly,
409 2,892,582 SNPs were called using samtools. Initial filtering with vcftools left 1,300,961
410 SNPs. Next, we created the missing data set (MDS) by leaving our SNPs as-is and an imputed
411 set (IDS) by imputing the MDS with Beagle. After filtering each set for monomorphic SNPs,
412 minor allele frequency, and Wright's F outliers, the MDS retained 778,406 SNPs while the IDS
413 retained 1,029,063 SNPs. We reduced each set further to include only the intersection of loci
414 between the data sets, resulting in two data sets (MDS, IDS) each with 713,745 SNPs. Finally,
415 we reduced these sets further by choosing from each contig in the MDS the SNP with the least
416 amount of missing data. In cases where multiple SNPs across the same contig were equal in
417 missing data, we chose randomly from this subset of SNPs. We then removed the remaining

418 SNPs on the contig from both IDS and MDS. After these filtering steps, we retained 116,231
419 SNPs from the IDS for use as the empirical set in downstream analyses (Table S1). Of these
420 contigs, 107,354 (92.4%) mapped to the *P. lambertiana* reference genome with 85% similarity
421 and 50% query length coverage thresholds, thus lending authenticity to our sequence data.
422 However, we avoid further discrimination of loci for (proximity to) genic regions until a future
423 genome update with increased curation and density of annotation.

424 Phenotypic traits were heritable and structured across populations – bud flush $h^2 = 0.3089$
425 $Q_{ST} = 0.0156$; $\delta^{13}\text{C}$ $h^2 = 0.7787$, $Q_{ST} = 0.0427$; height $h^2 = 0.0608$, $Q_{ST} = 0.0418$; $\delta^{15}\text{N}$ $h^2 =$
426 0.3525 , $Q_{ST} = 0.0191$; root:shoot $h^2 = 0.3240$, $Q_{ST} = 0.0110$; Table S4). Overall, populations
427 show little genetic structure with plots accounting for less than 1% of the variance in allele
428 frequencies ($F_{\text{plot,total}} = 0.00687$; 95% credible interval: 0.0067-0.0070). Of this variation, 56.6%
429 was accounted for by populations ($F_{\text{pop,total}} = 0.00389$; 95% CI: 0.0038-0.0040) with the
430 remainder due to plots within populations ($F_{\text{plot,pop}} = 0.00299$; 95% CI: 0.0029-0.0031). We
431 found similar patterns among the locus-specific estimates of F_{ST} (Figure S3). Moreover, we
432 found no discernable clustering of populations using PCA, respectively accounting for 5.6% and
433 1.2% of the variance in allele frequencies (Figure S11). To further address applicability of the
434 island model used for calculation of allelic covariance ($\hat{D}_{a(ij)}$) and allele frequency shifts
435 ($pw\hat{D}_{a(ij)}$) we analyzed population pairwise F_{ST} according to Weir and Cockerham (1984) using
436 the `hierfstat` package in R. Results show little differentiation among populations (mean =
437 0.005, max = 0.016) with no evidence of isolation by distance (Mantel's $r = 0.0990$, $p = 0.2310$).

438 **Genotype-environment analyses**

439 To explore the degree of association among environmental variables between populations,
440 we used Mantel tests between Euclidian environmental distance matrices. In most cases we
441 found significant correlations with many of the edaphic variables measured for this study, as
442 well as between latitude and elevation ($r = 0.3988$, $p = 0.0490$), longitude and annual

443 precipitation ($r = 0.7145$, $p = 0.0030$), and between percent maximum solar radiation and
444 latitude distances ($r = 0.4629$, $p = 0.0370$; Table 3). Additionally, geographic distance among
445 populations was only associated with latitude ($r = 0.9631$, $p = 0.001$), percent maximum solar
446 radiation input ($r = 0.3992$, $p = 0.0468$), and elevation ($r = 0.4062$, $p = 0.0452$), the three of
447 which were correlated environmentally (Table 3), but not to any of the remaining environmental
448 variables (Mantel tests $p > 0.3131$, data not shown).

449 Through the intersection of the top 0.5% of \overline{BF} and top 1% of $\overline{p_S}$, `bayenv2` analysis
450 revealed between 14 (CEC) and 157 (GDD-Aug) focal SNPs associated with environment
451 (Table 2). However, when calculating the \overline{BF} for each SNP, it was never the case that more
452 than two of the five chains produced $BF > 1$. The range of $\overline{p_S}$ across all focal SNPs across all
453 environments varied from a minimum of 0.138 to a maximum 0.345 (Table 2). Additionally, the
454 focal SNPs identified by `bayenv2` displayed a bias towards SNPs with low values of H_E
455 (Figures S1-S2) when compared to the distribution from the full set of SNPs (Figure S13). As
456 such, our environmental associations should be interpreted with caution, as we did not have any
457 SNPs with $\overline{BF} > 1$ nor do our nonparametric correlations exceed 0.35. Even so, when we
458 compared absolute estimates of allele frequency covariance ($\hat{D}_{a(ij)}$) among focal SNPs against
459 the corresponding 1000 sets of random SNPs (the null sets) equal in set size as well as within
460 H_E bins, we found that for all focal sets the median $\hat{D}_{a(ij)}$ was always greater than the 100th
461 percentile of the null distribution (Table 2). The magnitude of this difference varied across
462 environmental variables, being the smallest for percent clay (1.17x) and largest for annual
463 precipitation (5.10x, Table 2). The percentile of the focal $\hat{D}_{a(ij)}$ distribution corresponding to the
464 100th percentile of the associated null set varied across environmental variables as well,
465 reaching just the 3rd percentile for minimum January temperature and the 43rd percentile for
466 percent clay (Table 2), suggesting that for most environmental variables the focal SNPs show
467 higher degrees of covariance than expected by chance, despite having low \overline{BF} and $\overline{p_S}$.

468 Through the examination of patterns of allele frequency shifts ($pw\hat{D}_{a(ij)}$) across loci
469 associated with environment we found no significant associations with geographic distance
470 using Mantel tests ($p > 0.1116$, data not shown). While this suggests the absence of linear
471 allelic clines, it does not necessarily preclude the presence of environmental gradients or
472 correlated patches as suggested by environmental distance associations (Table 3). When we
473 investigated the association between allele frequency shift ($pw\hat{D}_{a(ij)}$) matrices against the
474 eponymous environmental distance matrix, we found significant association for annual
475 precipitation ($r = 0.7134$, $p = 0.0027$), GDD-May ($r = 0.8480$, $p = 0.0013$), longitude ($r = 0.6522$,
476 $p = 0.0024$), percent rock coverage ($r = 0.5124$, $p = 0.0145$), percent sand ($r = 0.5574$, $p =$
477 0.0046), minimum January temperature ($r = 0.5791$, $p = 0.0137$), and WC- $\frac{1}{3}$ bar (field capacity, r
478 $= 0.4806$, $p = 0.0361$; Table 5). Additionally, we examined relationships between a particular
479 $pw\hat{D}_{a(ij)}$ matrix and the 17 remaining environmental distance matrices and found significant
480 associations in an additional 13 comparisons (Table 5), with five of these comparisons having
481 $pw\hat{D}_{a(ij)}$ associated with either annual precipitation or longitudinal Euclidian distance. We also
482 observed shifts of alleles associated with longitude or soil water capacity across six of the
483 remaining eight significant associations (Table 5), with the remaining two significant
484 associations among edaphic conditions of sand, silt, or clay. The magnitude of the mean allele
485 frequency difference across populations of focal SNPs (range 0.018-0.029) were generally
486 larger than that predicted from random SNPs of the same heterozygosity (Figures S15-S16).
487 Overall, our results indicate that the vast majority of subtle allele frequency shifts among loci
488 associated with environment also have significant associations related to annual precipitation,
489 longitude, or available soil water capacity.

490 **Genotype-phenotype analyses**

491 We used a subset of the empirical set of SNPs for use in genotype-phenotype analysis to
492 account for only those populations with individuals contributing to the common garden ($n = 88$

493 trees, see Table 1). We filtered SNPs with MAF < 0.01 across these 6 populations to retain
494 115,632 SNPs. PCA revealed a similar pattern to the empirical set of SNPs (data not shown).
495 Using three significant axes of population structure identified through Tracy-Widom tests, we
496 associated SNPs to phenotypes with BSLMM (Zhou *et al.* 2013) using the top 99.9th and 99.8th
497 percentiles of \overline{PIP} (Table 4, Figure S4). From observations of density and trace plots, we con-
498 cluded that the posterior distributions across chains were converging (not shown). The H_E of
499 focal loci were generally representative of the empirical set (Figures S18-19). While the
500 phenotypic main effect ($\bar{\beta}$) of loci across \overline{PIP} sets ranged from 0-0.2 (Figure S5), the random
501 effects ($\bar{\alpha}$) and total effect ($\bar{\alpha} + \bar{\beta} * \overline{PIP}$) were generally well below 6e-04 (Figures S6-7)
502 suggestive of small effects of similar magnitude across focal loci.

503 Overall, the genetic variance of SNPs included in the polygenic model explained between
504 14.4% ($\delta^{15}\text{N}$) and 37.6% (root:shoot) of the variance in the phenotypes measured in our study
505 (PVE , Figure 2, Table S4). For many of the measured phenotypes, a considerable proportion of
506 the narrow sense heritability estimated previously (Table S4) was accounted for in the estimates
507 of PVE . Interestingly, in the case of height, PVE exceeded the upper confidence interval of the
508 estimated h^2 (Table S4). Even so, PVE estimates were subject to uncertainty, particularly
509 root:shoot biomass (Figure 2), and thus, PVE could be larger or smaller than estimated here.
510 Similarly, the estimates for the number of SNPs underlying the phenotype also showed
511 uncertainty, and we acknowledge that these estimates could be larger or smaller than that
512 estimated by the mean (Figure 2, Table S4).

513 To acquire estimates of PVE from the identification of loci with large effects on phenotype,
514 we conducted single-locus association using univariate linear mixed models implemented in
515 GEMMA (see Appendix, Table S2). Across all phenotypes, there were no loci that exceeded the
516 adjusted threshold for inclusion calculated from q -values with an FDR of 0.05 (Storey *et al.*
517 2015; v2.4.2), with the minimum q -value across SNPs within phenotypes ranging between

518 0.2046 ($\delta^{13}\text{C}$) and 0.9999 ($\delta^{15}\text{N}$) (Table S2). Except for root:shoot biomass, the maximum
519 likelihood estimates of *PVE* differed drastically from the estimates from BSLMM, with *PVE* never
520 exceeding $1.08\text{e-}06$ (Table S2) suggesting that a larger proportion of the heritable genetic
521 variation for the traits measured here is explained by multiple SNPs than by individual SNPs of
522 large effect. Finally, to determine if any relatively large-effect loci from the univariate LMMs that
523 were near the threshold were captured by the BSLMM for a particular phenotype, we isolated
524 the loci from univariate LMM above a reduced threshold of $-\ln(p_{\text{Wald}}) \geq 10$ (see Figure S10,
525 Appendix). By this reduced threshold we identified one unique locus for both bud flush and $\delta^{15}\text{N}$,
526 four unique loci for both height and root:shoot biomass, and five unique loci for $\delta^{13}\text{C}$ (15 unique
527 loci overall). We examined the focal loci sets identified from the 99.9th percentile of \overline{PTP} in
528 BSLMM for these LMM reduced-threshold loci and found 1/4 for both root:shoot biomass and
529 height, and 2/5 for $\delta^{13}\text{C}$. When we assessed the set of loci in the 99.8th percentile of BSLMM
530 \overline{PTP} , we recovered all LMM reduced-threshold loci for bud flush and $\delta^{15}\text{N}$ ($n = 1$), 1/4 loci for
531 root:shoot biomass, 3/4 loci for height, and 3/5 loci for $\delta^{13}\text{C}$.

532 To determine if focal loci associated with phenotype by BSLMM showed signatures of an
533 underlying polygenic architecture under selection, we estimated allele frequency covariance
534 ($\widehat{D}_{a(ij)}$) among focal SNPs and compared these estimates to 1000 sets of SNPs each randomly
535 sampled from H_E bins represented in the focal set. We found evidence for elevated covariance
536 among the 99.9th percentile of \overline{PTP} loci associated with bud flush and root:shoot biomass (Table
537 4), with the latter exceeding the 100th percentile of the random distribution. To consider larger
538 numbers of loci representative of the number of underlying loci estimated by BSLMM (Figure 2b,
539 Table S4), we also isolated SNPs from the top 99.8th percentile of \overline{PTP} . In this set we found
540 evidence for elevated covariance for all phenotypes except for height, which did not produce a
541 focal median $\widehat{D}_{a(ij)}$ greater than the 95th percentile of null distribution of $\widehat{D}_{a(ij)}$ (Table 4).

542 To identify signatures of allele frequency shifts among focal loci associated with

543 phenotype ($pw\hat{D}_{a(ij)}$), we ran mantel tests of $pw\hat{D}_{a(ij)}$ matrices against geographic distance and
544 environmental Euclidian distance matrices. When considering SNPs identified by the 99.9th
545 percentile of \overline{PTP} , we see substantial evidence for allele frequency shifts of loci associated with
546 bud flush to Euclidian distances of GDD-May, GDD-Aug, percent maximum radiation input, and
547 minimum January temperature (Table 6). Additionally, when we consider the 99.8th percentile of
548 \overline{PTP} , we show evidence for allele frequency shifts among loci associated with bud flush, height,
549 and $\delta^{13}\text{C}$ to Euclidian distances of annual precipitation, as well as for $\delta^{15}\text{N}$ loci to elevation, and
550 bud flush loci to both longitude (a correlate of annual precipitation) and to percent maximum
551 radiation input (as in the 99.9th \overline{PTP} set). The magnitude of the allele frequency differences
552 across populations were subtle (range: 0.054-0.087) and representative of unassociated SNPs
553 of similar H_E (Figure S17). Taken together, the lack of any significant large-effect loci, the low
554 PVE for univariate models compared with BSLMM, the covariance of allele frequencies among
555 associated SNPs, and the evidence for coordinated shifts in allele frequencies relative to
556 environmental distances (particularly to bud flush, soil water availability and correlated
557 environmental variables), our data suggests an overall polygenic basis of local adaptation.

558 *F_{ST}* outlier analysis

559 From the empirical set of SNPs $\text{Out}_{\text{FLANK}}$ analysis revealed 110 focal loci as outliers for
560 F'_{ST} (range: 0.069-0.118). Expected heterozygosity values among the outlier SNPs (Figure S14)
561 varied across nearly the entire distribution from the full set of SNPs (Figure S13). Upon analysis
562 of patterns of covariance ($\hat{D}_{a(ij)}$) among the $\text{Out}_{\text{FLANK}}$ focal SNPs against 1000 sets of random
563 SNPs equal in total set size as well as within expected heterozygosity bins (the null sets), we
564 found that the median focal $\hat{D}_{a(ij)}$ (6.08e-03) was 10.6x greater than the 100th percentile of the
565 null distribution of $\hat{D}_{a(ij)}$ (5.74e-04). Moreover, the maximum median $\hat{D}_{a(ij)}$ from null sets
566 corresponded to just the 12th percentile (743/5995, where $\binom{110}{2} = 5995$) of the focal $\hat{D}_{a(ij)}$
567 values, suggesting that the majority of SNPs within the focal set showed higher levels of

568 covariance among other outliers than expected by chance. However, when we analyzed these
569 outlier SNPs for signatures of allele frequency shifts ($pw\hat{D}_{a(ij)}$) we found no significant
570 associations with geographic or environmental distances.

571 *Intersection of SNPs within and across methods*

572 We examined overlap of focal SNPs among the various methods employed in this study
573 (Table S3). Overall there was more overlap of loci associated with multiple phenotypes or with
574 multiple environments than found across methods. For sets of loci associated with environ-
575 mental variables, there was a considerable number of loci that were found to overlap among
576 comparisons. This seemed to be driven by the correlations among environments, for when
577 ordered by the number of loci within the intersection, 12 of the top 15 comparisons were among
578 edaphic conditions. Overall, Out_{FLANK} captured 4 of the loci identified in the 99.8th percentile of
579 \overline{PTP} , between 1-3 of the loci identified across 10/18 environmental associations from *bayenv2*
580 (including annual precipitation), but not for any of the moderate-effect loci identified from the
581 reduced threshold of LMM. Among loci associated with phenotype (99.8th \overline{PTP}), there were
582 between one and three loci which were found in the intersection among pairwise phenotypic
583 comparisons, yet none of these loci were those identified from LMM. Very few of the loci
584 identified by *bayenv2* would have been detected through conventional F_{ST} outlier approaches
585 (Figures S8-9). Finally, there was little overlap among loci associated with environment with the
586 99.8th percentile of \overline{PTP} (including two between $\delta^{13}C$ and longitude) and environmental
587 associations did not capture any of the reduced-threshold loci from univariate LMM (Table S3).

588 **DISCUSSION**

589 The spatial extent of local adaptation, particularly in conifers, has generally been
590 investigated at regional scales using single-locus perspectives (Neale and Savolainen 2004;
591 Savolainen *et al.* 2007; Ćalić *et al.* 2016). While informative for range-wide inference,
592 management and conservation agencies are often limited to local scales spanning only several

593 to tens of square kilometers. While there is an expectation that high gene flow (i.e., migration
594 load) exhibited by many conifers can lead to swamping of adaptive alleles, there is mounting
595 empirical evidence that adaptation to the environment can still occur at relatively fine spatial
596 scales (Mitton 1989; 1999; Budde *et al.* 2014; Csilléry *et al.* 2014; Vizcaíno *et al.* 2014; Eckert *et*
597 *al.* 2015), particularly when the environment is highly heterogeneous and selective forces are
598 strong. Thus, studies which investigate adaptation at scales amenable to management may be
599 of relatively greater importance, especially for endangered and threatened species, for
600 reforestation applications such as those carried out through seed sourcing (*sensu* McLane and
601 Aitken 2012) and replanting efforts. Here, our results also highlight the advantage of a polygenic
602 perspective. For instance, through this approach we found that the degrees of covariance
603 among loci which may have been otherwise overlooked using a single locus perspective
604 (*bayenv2* loci with $\overline{BF} < 1$) tracked environmental distance often related to water availability, a
605 pattern corroborated by similar inferences gained from a multilocus approach to phenotypic
606 association. Together, this evidence lends replicative support to both recent and long-standing
607 theory for the patterns of loci underlying quantitative traits undergoing selection with gene flow.

608 ***Standing genetic variation for fitness-related traits***

609 The populations under study appear to have extensive gene flow, recent divergence, or
610 both. Variation of allele frequencies among populations accounts for less than 1% of the
611 variance observed, which was less than that found for *P. lambertiana* populations within the LTB
612 (Eckert *et al.* 2015), or among isozymes sampled from populations across the Northern *P.*
613 *albicaulis* range (Krakowski *et al.* 2003). Additionally, inspection of PCs showed no distinctive
614 clustering of populations (Figure S11) while population pairwise F_{ST} did not exceed 0.016 and a
615 test for isolation by distance was not significant. For focal SNPs identified by *bayenv2*, average
616 allele frequency differences between populations were generally slightly larger than for the
617 majority of SNPs in the null set (Figures S15-S16). Contrastingly, SNPs identified from GEMMA
618 were roughly representative of the average allele frequency differences from the null set (Figure

619 S17). The magnitude of allele frequency differences across populations of loci associated by
620 *bayenv2* may have been less than those associated by GEMMA due to reducing the sample size
621 to only trees contributing seedlings to the common garden. Biologically, this pattern of extensive
622 sharing of alleles across populations has likely resulted from a combination of long-distance
623 pollen movement and seed dispersal by Clark's nutcracker (*Nucifraga columbiana* Wilson)
624 which is known to disperse seeds at distances similar to those between our sampled
625 populations (Tomback 1982; Richardson *et al.* 2002 and references therein). Given this pattern
626 of structure, the island model with symmetric migration used to describe the interpopulation
627 component of linkage disequilibrium among loci ($\hat{D}_{a(ij)}$) and allele frequency shifts ($p_w \hat{D}_{a(ij)}$) is
628 likely suitable to investigate our dataset for signatures of polygenic adaptation.

629 *P. albicaulis* of the Lake Tahoe Basin exhibit substantial genetic variation for the fitness-
630 related traits measured (Figure 2), suggesting that ongoing adaptation within the LTB will likely
631 be unconstrained by the lack of genetic variation and instead by other factors such as
632 population growth (i.e., declination) rates. A much larger proportion of the heritable variation
633 (estimated in Maloney *et al. in review*) can be explained by multiple SNPs than by individual
634 SNPs of large effect. Together our analyses suggest that selection among the LTB populations
635 is acting through many loci of small to moderate effect (Figure 2, Table S4). As prolonged bouts
636 of selection with gene flow are expected to result in reduced variation through the concentration
637 of architectures with fewer, larger, and more strongly linked adaptive loci (Yeaman and Whitlock
638 2011), our results may also suggest that selection has been recent (relative to $4N_e$ generations).
639 During the Pleistocene-Holocene transition (10,000-12,000yr BP), shifts from mesic to xeric
640 conditions caused proximal *P. albicaulis* populations of the western Great Basin (~50km distant)
641 to shift from 1380m in elevation to their current position about 1100m down-slope (Nowak *et al.*
642 1994; *cf.* Table 1). Such shifts in climate and local edaphic conditions in the last 10,000yr may in
643 part explain a recent selective episode on *P. albicaulis* populations of the LTB.

644 ***Polygenic signals of local adaptation***

645 Studies of tree species have described adaptive loci showing evidence of moderate to
646 large effect on fitness-related traits (Neale and Savolainen 2004; Savolainen *et al.* 2007; Čalić
647 *et al.* 2016). Much of this work in this regard occurred across relatively large geographic scales
648 and generally without further description of signals predicted from an underlying polygenic
649 basis. In contrast, Ma *et al.* (2010) assessed evidence for diversifying selection within European
650 aspen (*Populus tremula* L.) across 23 candidate genes of the photoperiodic pathway using the
651 covariance of allelic effects among loci, albeit across a geographic region of Sweden spanning
652 10 latitudinal degrees. From this candidate set, they identified high degrees of covariance
653 among phenotypic effects as predicted from theory (Latta 1998), despite minimal allele
654 frequency differentiation among sampled populations. More recently, Csilléry *et al.* (2014)
655 assessed 53 climate-related candidate genes within European beech (*Fagus sylvatica* L.)
656 providing evidence that covariance among loci is attributable to epistatic selection (*sensu* Ohta
657 1982) across short spatial scales. While varying across spatial scales, they replicate evidence
658 for a polygenic signal of local adaptation through linkage disequilibrium among adaptive loci.

659 Although we expected to uncover some alleles with relatively large effect, a polygenic archi-
660 tecture for the measured fitness-related traits was expected, given the multifaceted and quant-
661 itative nature of these traits. With levels of high covariance of allele frequencies among loci
662 associated with phenotypes, environment, and genetic differentiation, our results corroborate
663 this expectation. For example, loci associated with phenotype ($\geq 99.8^{\text{th}}$ percentile \overline{PIP}) showed
664 high covariance for all traits except for height (Table 4), while all cases with `OutFLANK` and
665 `bayenv2`, the median levels of covariance among focal SNPs were between 1.17-10.6x greater
666 than the 100th percentile of the null distribution (Table 2, Results). This suggests that the
667 covariance among these identified loci was greater than expected by chance. However, the low
668 levels of expected heterozygosity among SNPs associated with environment were unexpected
669 (Figures S1-S2). To explore this bias, we examined uncorrected correlations among allelic

670 frequencies and environmental measures. From this, we found no apparent pattern between
671 expected heterozygosity and environmental correlation across the whole dataset, within the top
672 SNPs correlated to environment (same N as identified by `bayenv2`), the top 500 SNPs, or
673 through the inclusion of an over-representation of loci with large H_E among these three sets of
674 SNPs (data not shown). This suggests that loci of greater H_E weren't excluded from association
675 because they contained more information regarding demographic structure or that the `bayenv2`
676 analyses were driven by statistical outliers. Even so, `bayenv2` did not identify any loci strongly
677 associated with environment, as given from small values of Bayes factors (all $\overline{BF} < 1.0$, Table
678 2), which is consistent with an underlying architecture with many loci of small effect. Yet, given
679 the strong biological signal for adaptation to soil water availability in our dataset (discussed
680 below), as well as evidence that other white pines within the LTB are also being structured by
681 precipitation differences among populations (Eckert *et al.* 2015), it seems unlikely that the focal
682 sets of SNPs are driven by false positives. However, if the majority of loci across `bayenv2` are
683 true positives and not an artifact of the method, one possible explanation for elevated
684 covariance among focal loci is that the structure of environmental variables across populations
685 captured variation for unmeasured phenotypic traits which were largely representative of total
686 lifetime fitness (Schoville *et al.* 2012). Structure of unmeasured fitness-related traits could also
687 explain the high covariance of `OutFLANK` loci. Future work could provide validation through
688 functional analyses of loci or from similar patterns found in other systems.

689 The strongest signal for local adaptation among *P. albicaulis* populations of the LTB
690 came from evidence of adaptation to soil water availability, as well as other environmental
691 variables correlated with annual precipitation (e.g., longitude; see Figure 1). For example, water-
692 use efficiency as measured by $\delta^{13}\text{C}$ was one of the phenotypes with loci that exhibited high
693 levels of covariance (Table 4). Our results provide evidence that the covariance of allele
694 frequencies among adaptive loci is also tracking soil moisture conditions among the studied
695 populations. Of the six significant associations between population pairwise environmental

696 distance and allele frequency shifts ($pw\hat{D}_{a(ij)}$) of loci associated with phenotype, four were
697 related to annual precipitation or longitude where $\delta^{13}\text{C } pw\hat{D}_{a(ij)}$ itself was associated with
698 interpopulation differences in annual precipitation (Table 6), including height, which did not
699 exhibit elevated covariance among associated loci (Table 4). Of the loci associated with
700 environment, both annual precipitation and longitudinal $pw\hat{D}_{a(ij)}$ were among those ($n = 7$)
701 associated with the eponymous environmental distance while, of the 13 non-eponymous
702 associations, 11 were related with annual precipitation, longitude, or soil water capacity (Table
703 5). Together, this evidence suggests that *P. albicaulis* populations are undergoing selection for
704 soil water availability limits across the LTB despite high levels of gene flow.

705 ***Water availability as a driver of local adaptation***

706 Water availability is a critical component shaping standing variation across plant taxa
707 (Vicente-Serrano *et al.* 2013), including the distributions of tree species in general (van
708 Mantgem *et al.* 2009; Allen 2010), and southern populations of *P. albicaulis* specifically (Bower
709 and Aitken 2008; Chang *et al.* 2014). Because of climatic constraints imposed on the southern
710 range of *P. albicaulis*, phenotypic traits which are correlated to precipitation, soil water
711 availability, or soil water capacity likely have fitness-related consequences for this species. With
712 climatic models predicting warmer temperatures, reduced snow accumulation, and earlier spring
713 melt across the western USA, it is likely that *P. albicaulis* populations of the Sierra Nevada will
714 continue to face continuing selective pressures of this kind.

715 Past research regarding variation in $\delta^{13}\text{C}$ among conifers has shown that this trait
716 displays substantial levels of heritability across species (Seiler and Johnson 1988; Cregg 1993;
717 Brendel *et al.* 2002; Baltunis *et al.* 2008; Cumbie *et al.* 2011; Eckert *et al.* 2015), and consists of
718 a polygenic architecture with constituent loci being comprised of both large and small effect
719 (Brendel *et al.* 2002; González-Martínez *et al.* 2008; Cumbie *et al.* 2011; Marguerit *et al.* 2014).
720 Indeed, we have found significant heritability for the measured phenotypes with the observed

721 phenotypic variation (Q_{ST}) structured across populations (Table S4; Maloney *et al. in review*).
722 Here, we have found segregating genetic variation of a polygenic architecture that explains a
723 considerable portion of the heritability for this trait (Table S4). Additionally, there was a
724 significant association between phenotypic differences of $\delta^{13}\text{C}$ and $\delta^{15}\text{N}$ (Table 3), which have
725 been noted in other species such as *P. taeda* L. (Cumbie *et al.* 2011) and *P. lambertiana*
726 (Eckert *et al.* 2015). This suggests that studied populations of *P. albicaulis* are capable of
727 maximizing nitrogen-use efficiency under low availability of water (e.g., Livingston *et al.* 1999)
728 and perhaps that water-use efficiency is determined through leaf assimilation to a larger extent
729 than stomatal conductance (e.g., Prasolova *et al.* 2005). While we did not measure pleiotropy
730 directly (as in Gompert *et al.* 2015), and despite the association, $\delta^{13}\text{C}$ and $\delta^{15}\text{N}$ shared just one
731 focal locus (Table S3). Because this locus was not one of those identified from the relaxed
732 thresholds for the univariate LMM, it is possible that this locus has a minor effect on either trait.

733 **Concluding remarks, limitations, and future work**

734 The results reported here suggest that the genetic architecture for variation in fitness-related
735 phenotypic traits of *P. albicaulis* consists of numerous loci of small to moderate effects, that
736 these loci show higher covariance than expected by chance, and that this covariance is often
737 associated with interpopulation levels of soil water availability. Our results further explain a
738 considerable portion (*PVE*) of the additive genetic variation (h^2) of the quantitative traits under
739 study from a polygenic perspective. Thus, we can posit that the general mode of adaptation for
740 *P. albicaulis* across the LTB is facilitated by selection on standing levels of genetic variation that
741 is extensively shared throughout the basin and likely improves performance in early life stages.
742 Finally, if soil and climatic variables continue to influence the extant populations within the LTB
743 as evidenced from our analyses, it is likely that these variables will continue to be important to
744 the long term success of this threatened keystone species.

745 While we described associations among genotype, phenotype, and environment that reflect

746 strong evidence for adaptive responses of *P. albicaulis* populations to the environment, we
747 acknowledge several shortcomings. First, our study design was limited in statistical power which
748 could have been improved by increasing the number of individuals sampled, the total number of
749 populations, or both, given an ideal sampling regime (Lotterhos and Whitlock 2015). Second,
750 while we measured fitness-related traits among seedlings of a species whose lifespan differs by
751 several orders of magnitude, establishment success is one of the primary factors influencing
752 dynamics of forest populations and is most likely a major component of total lifetime fitness.
753 Third, much of the statistical signal for the association of allele frequency shifts to environment
754 would be lost with correction for multiple tests yet we leverage the fact that, of the few significant
755 associations, the majority were related to $\delta^{13}\text{C}$, annual precipitation, its correlate of longitude, or
756 soil water capacity, an outcome highly unlikely by chance alone. Fourth, while we provide
757 evidence for statistical signals predicted by theory, our methodology limited us from making
758 conclusions regarding local adaptation *sensu stricto* as we utilized just a single common garden
759 without reciprocal transplants and were unable to quantify functional differences of putative loci
760 among populations. Reciprocal transplants would have allowed us to differentiate pleiotropic
761 effects and facilitate direct measures of fitness through survival and growth across
762 environments. Finally, a more fully curated, well-annotated genome assembly and
763 accompanying linkage map would have aided in the detection of physical linkage among SNPs,
764 proximity to genomic regions of estimated effect, (non)synonymous mutations, and detection of
765 false positives. For instance, the *P. lambertiana* genome used to judge authenticity of sequence
766 data does not yet have the density of annotation needed to draw inferences on the causative
767 sites likely within or linked to the loci described here, as its assembly and curation are still
768 ongoing. Because of this, we cannot confidently estimate the proportion of the polymorphism
769 due to coding and non-coding sites nor conclude that the relatively small effects inferred for
770 focal loci are not an artifact due to distant linkage with causative sites of larger effect. Future
771 work could address these shortcomings and lead to the corroboration of our results, particularly

772 in describing patterns exhibited by underlying loci in other systems. However, while considered
773 an inconsistency by some (Ćalić *et al.* 2016), we have doubts as to whether the loci of small
774 effect uncovered here would show consistent discovery across conifer species, for when
775 adaptation occurs in the face of gene flow the architecture itself is often transient (Yeaman
776 2015), as no locus makes any considerable contribution for an extended period of time. Even for
777 such cases of loci of large effect, the genetic architecture of local adaptation can be transient if
778 genetic redundancies and effective mutation rates are high.

779 Lastly, we highlight calls from others (e.g., Pritchard and di Rienzo 2010; Sork *et al.* 2013;
780 Csilléry *et al.* 2014; Tiffin and Ross-Ibarra 2014; Hornoy *et al.* 2015; Stephan 2015; Tigano and
781 Friesen 2016) for future investigations into the genetic architectures of local adaptation of
782 fitness-related traits to continue to address a multilocus perspective and we relate this to a
783 recent meeting conferring forest tree genomic scientists (Groover 2015). There, delegates
784 identified challenges facing the advancement of insight into forest biology. While improvements
785 in computational, genomic, and sequencing technologies will continue to aid the capacity of
786 research, delegates specified that it would be the untested hypotheses that will bring about the
787 most fruitful insight. However, for this to take place, empiricism will need to continue to test
788 hypotheses currently at hand, as well as to develop and improve our overall evolutionary
789 understanding. With this, advances in the expectations of polygenic adaptation through theory
790 (of e.g., the effect of recombination, LD, genomic networks, as well as anisotropic gene flow or
791 selection pressures on the prediction of transient dynamics of small-effect alleles and genomic
792 clustering via rearrangement) will inform study and sampling design across spatial scales and
793 provide new and interesting models with which to contrast to evolving populations in nature.

794 **Acknowledgements**

795 We thank Annette Delfino Mix, Camille Jensen, Tom Burt, and Randi Famula for field, common
796 garden, and lab assistance. Additionally, we thank David Fournier, Joey Keely, Kurt Teuber
797 (USDA Forest Service - LTBMU), Roland Shaw (Nevada Division of Forestry), Bill Champion
798 (Nevada State Parks), Woody Loftis (USDA NRCS) for site information and permission to work
799 on Federal and State lands, the VCU CHiPC for computational resources, Jennifer Ciminelli for
800 GIS tips, and Lindsay Miles who helped improve this manuscript. This work was supported by
801 the Southern Nevada Public Lands Management Act – Rounds 7 and 10, sponsored by the
802 USDA, Forest Service, Pacific Southwest Research Station, Albany, CA.

803

REFERENCES

804 Allen C. D., Macalady A. K., Chenchouni H., Bachelet D., McDowell N., Vennetier M., Kitzberger

805 T., Rigling A., Breshears D. D., Hogg E. H. T., Gonzalez P., Fensham R., Zhang Z., Castro

806 J., Demidova N., Lim J.-H., Allard G., Running S. W., Semerci A., Cobb N., 2010 A global

807 overview of drought and heat-induced tree mortality reveals emerging climate change risks

808 for forests. *Forest Ecology and Management* **259**: 660–684.

809 Baltunis B. S., Martin T. A., Huber D. A., Davis J. M., 2008 Inheritance of foliar stable carbon

810 isotope discrimination and third-year height in *Pinus taeda* clones on contrasting sites in

811 Florida and Georgia. *Tree Genetics & Genomes* **4**: 797–807.

812 Barrett R., Schluter D., 2008 Adaptation from standing genetic variation. *Trends in Ecology &*

813 *Evolution* **23**: 38–44.

814 Barton N. H., 1999 Clines in polygenic traits. *Genetical Research* **74**: 223–236.

815 Bourret V., Dionne M., Bernatchez L., 2014 Detecting genotypic changes associated with

816 selective mortality at sea in Atlantic salmon: polygenic multilocus analysis surpasses

817 genome scan. *Molecular Ecology* **23**: 4444–4457.

818 Bower A. D., Aitken S. N., 2008 Ecological genetics and seed transfer guidelines for *Pinus*

819 *albicaulis* (Pinaceae). *American Journal of Botany* **95**: 66–76.

820 Brendel O., Pot D., Plomion C., Rozenberg P., Guehl J. M., 2002 Genetic parameters and QTL

821 analysis of $\delta^{13}\text{C}$ and ring width in maritime pine. *Plant, Cell & Environment* **25**: 945–953.

822 Browning B. L., Browning S. R., 2016 Genotype imputation with millions of reference samples.

823 *The American Journal of Human Genetics* **98**: 116–126.

824 Budde K. B., Heuertz M., Hernández-Serrano A., Pausas J. G., Vendramin G. G., Verdú M.,

- 825 González-Martínez S. C., 2014 In situ genetic association for serotiny, a fire-related trait, in
826 Mediterranean maritime pine (*Pinus pinaster*). *New Phytologist* **201**: 230–241.
- 827 Čalić I., Bussotti F., Martínez-García P. J., Neale D. B., 2015 Recent landscape genomics
828 studies in forest trees. *Tree Genetics & Genomes* **12**: 1–7.
- 829 Chang T., Hansen A. J., Piekielek N., 2014 Patterns and Variability of Projected Bioclimatic
830 Habitat for *Pinus albicaulis* in the Greater Yellowstone Area (B Bond-Lamberty, Ed.). *PLoS*
831 *ONE* **9**: e111669.
- 832 Comeault A. A., Flaxman S. M., Riesch R., Curran E., Soria-Carrasco V., Gompert Z., Farkas T.
833 E., Muschick M., Parchman T. L., Schwander T., Slate J., Nosil P., 2015 Selection on a
834 genetic polymorphism counteracts ecological speciation in a stick insect. *Current Biology*
835 **25**: 1975–1981.
- 836 Comeault A. A., Soria-Carrasco V., Gompert Z., Farkas T. E., Buerkle C. A., Parchman T. L.,
837 Nosil P., 2014 Genome-wide association mapping of phenotypic traits subject to a range of
838 intensities of natural selection in *Timema cristinae*. *The American Naturalist* **183**: 711–727.
- 839 Coop G., Witonsky D., Di Rienzo A., Pritchard J. K., 2010 Using environmental correlations to
840 identify loci underlying local adaptation. *Genetics* **185**: 1411–1423.
- 841 Cregg B. M., 1993 Seed-source variation in water relations, gas exchange, and needle
842 morphology of mature ponderosa pine trees. *Canadian Journal of Forest Research* **23**:
843 749–755.
- 844 Critchfield W. B., Little E. L., 1966 Geographic distribution of the pines of the world (No. 991).
845 US Department of Agriculture, Forest Service.
- 846 Csilléry K., Lalagüe H., Vendramin G. G., González-Martínez S. C., Fady B., Oddou-Muratorio

- 847 S., 2014 Detecting short spatial scale local adaptation and epistatic selection in climate-
848 related candidate genes in European beech (*Fagus sylvatica*) populations. *Molecular*
849 *Ecology* **23**: 4696–4708.
- 850 Cumbie W. P., Eckert A. J., Wegrzyn J., Whetten R., Neale D., Goldfarb B., 2011 Association
851 genetics of carbon isotope discrimination, height and foliar nitrogen in a natural population
852 of *Pinus taeda* L. *Heredity* **107**: 105–114.
- 853 Daly C., Neilson R. P., Phillips D. L., 1994 A statistical-topographic model for mapping
854 climatological precipitation over mountainous terrain. *Journal of Applied Meteorology* **33**:
855 140–158.
- 856 Danecek P., Auton A., Abecasis G., Albers C. A., Banks E., DePristo M. A., Handsaker R. E.,
857 Lunter G., Marth G. T., Sherry S. T., others, 2011 The variant call format and VCFtools.
858 *Bioinformatics* **27**: 2156–2158.
- 859 East E. M., 1910 A Mendelian interpretation of variation that is apparently continuous. *The*
860 *American Naturalist* **44**: 65–82.
- 861 Eckert A. J., Maloney P. E., Vogler D. R., Jensen C. E., Mix A. D., Neale D. B., 2015 Local
862 adaptation at fine spatial scales: an example from sugar pine (*Pinus lambertiana*,
863 *Pinaceae*). *Tree Genetics & Genomes* **11**: 42.
- 864 Eckert A. J., van Heerwaarden J., Wegrzyn J. L., Nelson C. D., Ross-Ibarra J., González-
865 Martínez S. C., Neale D. B., 2010 Patterns of population structure and environmental
866 associations to aridity across the range of loblolly pine (*Pinus taeda* L., *Pinaceae*). *Genetics*
867 **185**: 969–982.
- 868 Eckert A. J., Wegrzyn J. L., Pande B., Jermstad K. D., Lee J. M., Liechty J. D., Tearse B. R.,

- 869 Krutovsky K. V., Neale D. B., 2009 Multilocus patterns of nucleotide diversity and
870 divergence reveal positive selection at candidate genes related to cold hardiness in coastal
871 douglas fir (*Pseudotsuga menziesii* var. *menziesii*). *Genetics* **183**: 289–298.
- 872 Ehret G. B., Lamparter D., Hoggart C. J., Whittaker J. C., Beckmann J. S., Kutalik Z.,
873 Consortium G. I. O. A. T., 2012 A multi-SNP locus-association method reveals a substantial
874 fraction of the missing heritability. *The American Journal of Human Genetics* **91**: 863–871.
- 875 Ellison A. M., Bank M. S., Barton D. C., Colburn E. A., Elliot K., Ford C. R., Foster D. R.,
876 Kloeppel B. D., Knoepp J. D., Lovett G. M., Mohan J., 2005 Loss of foundation species:
877 consequences for the structure and dynamics of forested ecosystems. *Frontiers in Ecology*
878 *and the Environment* **3**: 479-486.
- 879 Endler J. A., 1977 *Geographic variation, speciation, and clines*. No. 10, Princeton University
880 Press.
- 881 Farnes P. E., 1990 SNOTEL and snow course data: describing the hydrology of whitebark pine
882 ecosystems. General Technical Report INT (USA).
- 883 Fisher R. A., 1918 The correlation between relatives on the supposition of Mendelian
884 inheritance. *Transactions of the Royal Society of Edinburgh* **52**: 399–433.
- 885 Fisher R. A., 1930 *The genetical theory of natural selection*. Oxford University Press.
- 886 Gladman S., Seeman T., 2016 Velvet Optimiser v2.5.5, available online
887 <http://bioinformatics.net.au/software.velvetoptimiser.shtml>.
- 888 Gompert Z., Jahner J. P., Scholl C. F., Wilson J. S., Lucas L. K., Soria-Carrasco V., Fordyce J.
889 A., Nice C. C., Buerkle C. A., Forister M. L., 2015 The evolution of novel host use is unlikely
890 to be constrained by trade-offs or a lack of genetic variation. *Molecular Ecology* **24**: 2777–

- 891 2793.
- 892 González-Martínez S. C., Huber D., Ersoz E., Davis J. M., Neale D. B., 2008 Association
893 genetics in *Pinus taeda* L. II. Carbon isotope discrimination. *Heredity* **101**: 19–26.
- 894 Groover A., 2015 Genomic science provides new insights into the biology of forest trees. *New*
895 *Phytologist* **208**: 302–305.
- 896 Guan Y., Stephens M., 2011 Bayesian variable selection regression for genome-wide
897 association studies and other large-scale problems. *Annals of Applied Statistics* **5**: 1780–
898 1815.
- 899 Günther T., Coop G., 2013 Robust identification of local adaptation from allele frequencies.
900 *Genetics* **195**: 205–220.
- 901 Haasl R. J., Payseur B. A., 2016 Fifteen years of genomewide scans for selection: trends,
902 lessons and unaddressed genetic sources of complication. *Molecular Ecology* **25**: 5–23.
- 903 Hall D., Luquez V., Garcia V. M., St Onge K. R., Jansson S., Ingvarsson P. K., 2007 Adaptive
904 population differentiation in phenology across a latitudinal gradient in European aspen
905 (*Populus tremula*, L.): A comparison of neutral markers, candidate genes, and phenotypic
906 traits. *Evolution* **61**: 2849–2860.
- 907 Hereford J., 2009 A Quantitative Survey of Local Adaptation and Fitness Trade-Offs. *The*
908 *American Naturalist* **173**: 579–588.
- 909 Hermisson J., 2005 Soft sweeps: molecular population genetics of adaptation from standing
910 genetic variation. *Genetics* **169**: 2335–2352.
- 911 Holland J., 2007 Genetic architecture of complex traits in plants. *Current Opinion in Plant*

- 912 Biology **10**: 156–161.
- 913 Hornoy B., Pavy N., Gérardi S., Beaulieu J., Bousquet J., 2015 Genetic Adaptation to Climate in
914 White Spruce Involves Small to Moderate Allele Frequency Shifts in Functionally Diverse
915 Genes. *Genome Biology and Evolution* **7**: 3269–3285.
- 916 Hutchins H. E., Lanner R. M., 1982 The central role of Clark’s nutcracker in the dispersal and
917 establishment of whitebark pine. *Oecologia* **55**: 797-807.
- 918 Kemper K. E., Saxton S. J., Bolormaa S., Hayes B. J., Goddard M. E., 2014 Selection for
919 complex traits leaves little or no classic signatures of selection. *BMC Genomics* **15**: 246–
920 260.
- 921 Krakowski J., Aitken S. N., El-Kassaby Y. A., 2003 Inbreeding and conservation genetics in
922 whitebark pine. *Conservation Genetics* **4**: 581–593.
- 923 Kremer A., Le Corre V., 2012 Decoupling of differentiation between traits and their underlying
924 genes in response to divergent selection. *Heredity* **108**: 375–385.
- 925 Langlet O., 1971 Two hundred years of genecology. *Taxon*: 653–721.
- 926 Langmead B., Salzberg S. L., 2012 Fast gapped-read alignment with Bowtie 2. *Nature Methods*
927 **9**: 357–359.
- 928 Latta R. G., 1998 Differentiation of allelic frequencies at quantitative trait loci affecting locally
929 adaptive traits. *The American Naturalist* **151**: 283–292.
- 930 Latta R. G., 2003 Gene flow, adaptive population divergence and comparative population
931 structure across loci. *New Phytologist* **161**: 51–58.
- 932 Le Corre V., Kremer A., 2003 Genetic variability at neutral markers, quantitative trait loci and

- 933 trait in a subdivided population under selection. *Genetics* **164**: 1205–1219.
- 934 Le Corre V., Kremer A., 2012 The genetic differentiation at quantitative trait loci under local
935 adaptation. *Molecular Ecology* **21**: 1548–1566.
- 936 Leimu R., Fischer M., 2008 A meta-analysis of local adaptation in plants. *PLoS ONE* **3**: e4010.
- 937 Li H., Handsaker B., Wysoker A., Fennell T., Ruan J., Homer N., Marth G., Abecasis G., Durbin
938 R., 1000 Genome Project Data Processing Subgroup, 2009 The sequence alignment/map
939 format and SAMtools. *Bioinformatics* **25**: 2078–2079.
- 940 Livingston N. J., Guy R. D., Sun Z. J., 1999 The effects of nitrogen stress on the stable carbon
941 isotope composition, productivity and water use efficiency of white spruce (*Picea glauca*
942 (Moench) Voss). *Plant* **22**: 281–289.
- 943 Lotterhos K. E., Whitlock M. C., 2015 The relative power of genome scans to detect local
944 adaptation depends on sampling design and statistical method. *Molecular Ecology* **24**:
945 1031–1046.
- 946 Luquez V., Hall D., Albrechtsen B. R., Karlsson J., Ingvarsson P., Jansson S., 2007 Natural
947 phenological variation in aspen (*Populus tremula*): the SwAsp collection. *Tree Genetics &*
948 *Genomes* **4**: 279–292.
- 949 Ma X. F., Hall D., Onge K. R. S., Jansson S., Ingvarsson P. K., 2010 Genetic differentiation,
950 clinal variation and phenotypic associations with growth cessation across the *Populus*
951 *tremula* photoperiodic pathway. *Genetics* **186**: 1033–1044.
- 952 Mackay T. F. C., Stone E. A., Ayroles J. F., 2009 The genetics of quantitative traits: challenges
953 and prospects. *Nature Reviews Genetics* **10**: 565–577.

- 954 Mahalovich M. F., Stritch L., 2013 *Pinus albicaulis*. The IUCN Red List of Threatened Species.
955 e.T39049A2885918. <http://dx.doi.org/10.2305/IUCN.UK.2013-1.RLTS.T39049A2885918.en>.
- 956 Maloney P. E., Vogler D. R., Eckert A. J., Jensen C. E., Delfino-Mix A., (in review) Ecological
957 genetics of three white pine species from the Lake Tahoe Basin, USA: Implications for
958 conservation and evolutionary potential. 1–67.
- 959 Mantel N., 1967 The detection of disease clustering and a generalized regression approach.
960 *Cancer research* **27**: 209–220.
- 961 Marguerit E., Bouffier L., Chancerel E., Costa P., Lagane F., Guehl J. M., Plomion C., Brendel
962 O., 2014 The genetics of water-use efficiency and its relation to growth in maritime pine.
963 *Journal of Experimental Botany* **65**: 4757–4768.
- 964 McKay J. K., Latta R. G., 2002 Adaptive population divergence: markers, QTL and traits. *Trends*
965 *in Ecology & Evolution* **17**: 285–291.
- 966 McKinney S. T., Fiedler C. E., Tomback D. F., 2009 Invasive pathogen threatens bird-pine
967 mutualism: implications for sustaining a high-elevation ecosystem. *Ecological Applications*
968 **19**: 597-607.
- 969 McLane S. C., Aitken S. N., 2012 Whitebark pine (*Pinus albicaulis*) assisted migration potential:
970 testing establishment north of the species range. *Ecological Applications* **22**: 142–153.
- 971 Mitton J. B., Grant M. C., Yoshino A. M., 1998 Variation in allozymes and stomatal size in
972 pinyon (*Pinus edulis*, Pinaceae), associated with soil moisture. *American Journal of Botany*
973 **85**: 1262–1265.
- 974 Mitton J. B., Stutz H. P., Schuster W. S., 1989 Genotypic differentiation at PGM in Engelmann
975 spruce from wet and dry sites. *Silvae Genetica* **38**: 217–221.

- 976 Moser G., Lee S. H., Hayes B. J., Goddard M. E., Wray N. R., Visscher P. M., 2015
977 Simultaneous Discovery, Estimation and Prediction Analysis of Complex Traits Using a
978 Bayesian Mixture Model. *PLoS Genetics* **11**: e1004969.
- 979 Nowak C. L., Nowak R. S., Tausch R. J., Wigand P. E., 1994 A 30000 year record of vegetation
980 dynamics at a semi-arid locale in the Great Basin. *Journal of Vegetation Science* **5**: 579-
981 590.
- 982 Neale D. B., Savolainen O., 2004 Association genetics of complex traits in conifers. *Trends in*
983 *Plant Science* **9**: 325–330.
- 984 Nilsson-Ehle H., 1909 Kreuzungsuntersuchungen an Hafer und Weizen. *Lunds Universitets*
985 *Arsskrift* **5**: 1–122.
- 986 Ohta T., 1982 Linkage disequilibrium with the island model. *Genetics* **101**: 139–155.
- 987 Parchman T. L., Gompert Z., Mudge J., Schilkey F. D., Benkman C. W., Buerkle C. A., 2012
988 Genome-wide association genetics of an adaptive trait in lodgepole pine. *Molecular Ecology*
989 **21**: 2991–3005.
- 990 Pérez F., Granger B. E., 2007 IPython: A system for interactive scientific computing. *Computing*
991 *in Science and Engineering* **9**: 21-29.
- 992 Patterson N., Price A. L., Reich D., 2006 Population structure and eigenanalysis. *PLoS*
993 *Genetics* **2**: e190.
- 994 Peterson B. K., Weber J. N., Kay E. H., Fisher H. S., Hoekstra H. E., 2012 Double digest
995 RADseq: An inexpensive method for de novo SNP discovery and genotyping in model and
996 non-model species. *PLoS ONE* **7**: e37135.

- 997 Prasolova N. V., Xu Z. H., Lundkvist K., 2005 Genetic variation in foliar nutrient concentration in
998 relation to foliar carbon isotope composition and tree growth with clones of the F1 hybrid
999 between slash pine and Caribbean pine. *Forest Ecology and Management* **210**: 173–191.
- 1000 Pritchard J. K., Di Rienzo A., 2010 Adaptation – not by sweeps alone. *Nature Reviews Genetics*
1001 **11**: 665–667.
- 1002 R Core Team, 2015 R: A language and environment for statistical computing. R Foundation for
1003 Statistical Computing, Vienna, Austria. URL <http://www.R-project.org/>.
- 1004 Richardson B. A., Brunfeldt S. J., Klopfenstein N. B., 2002 DNA from bird-dispersed seed and
1005 wind-disseminated pollen provides insights into postglacial colonization and population
1006 genetic structure of whitebark pine (*Pinus albicaulis*). *Molecular Ecology* **11**: 215-227.
- 1007 Richardson J. L., Urban M. C., Bolnick D. I., Skelly D. K., 2014 Microgeographic adaptation and
1008 the spatial scale of evolution. *Trends in Ecology & Evolution* **29**: 165–176.
- 1009 Savolainen O., Lascoux M., Merilä J., 2013 Ecological genomics of local adaptation. *Nature*
1010 *Reviews Genetics* **14**: 807–820.
- 1011 Savolainen O., Pyhäjärvi T., Knürr T., 2007 Gene Flow and Local Adaptation in Trees. *Annual*
1012 *Review of Ecology, Evolution, and Systematics* **38**: 595–619.
- 1013 Schoville S. D., Bonin A., Francois O., Lobreaux S., Melodelima C., Manel S., 2012 Adaptive
1014 Genetic Variation on the Landscape: Methods and Cases. *Annual Review of Ecology,*
1015 *Evolution, and Systematics* **43**: 23–43.
- 1016 Seiler J. R., Johnson J. D., 1988 Physiological and morphological responses of three half-sib
1017 families of loblolly pine to water-stress conditioning. *Forest Science* **34**: 487–495.

- 1018 Sork V. L., Aitken S. N., Dyer R. J., Eckert A. J., Legendre P., Neale D. B., 2013 Putting the
1019 landscape into the genomics of trees: approaches for understanding local adaptation and
1020 population responses to changing climate. *Tree Genetics & Genomes* **9**: 901–911.
- 1021 Stephan W., 2015 Signatures of positive selection: from selective sweeps at individual loci to
1022 subtle allele frequency changes in polygenic adaptation. *Molecular Ecology* **25**: 79–88.
- 1023 Storey, J. D., Bass A. J., Dabney A., Robinson D., 2015 qvalue: Q-value estimation for false
1024 discovery rate control. R package version 2.4.2.
- 1025 Storz J. F., 2005 Using genome scans of DNA polymorphism to infer adaptive population
1026 divergence. *Molecular Ecology* **14**: 671–688.
- 1027 Storz J. F., Kelly J. K., 2008 Effects of spatially varying selection on nucleotide diversity and
1028 linkage disequilibrium: Insights from deer mouse globin genes. *Genetics* **180**: 367–379.
- 1029 Tiffin P., Ross-Ibarra J., 2014 Advances and limits of using population genetics to understand
1030 local adaptation. *Trends in Ecology & Evolution* **29**: 673–680.
- 1031 Tigano A., Friesen V. L., 2016 Genomics of local adaptation with gene flow. *Molecular Ecology*
1032 *AOP*: 1-21.
- 1033 Tomback D. F., 1982 Dispersal of whitebark pine seeds by Clark's nutcracker: a mutualism
1034 hypothesis. *The Journal of Animal Ecology* **51**: 451–467.
- 1035 Tomback D. F., Achuff P., 2010 Blister rust and western forest biodiversity: ecology, values and
1036 outlook for white pines. *Forest Pathology* **40**: 186-225.
- 1037 Tomback D. F., Arno, S.F, Keane R. E., 2001 Whitebark pine communities: ecology and
1038 restoration. Island Press, Washington, DC.

- 1039 Tomback D. F., Resler L. M., Keane R. E., Pansing E. R., Andrade A. J., Wagner A. C., 2016
1040 Community structure, biodiversity, and ecosystem services in treeline whitebark pine
1041 communities: potential impacts from a non-native pathogen. *Forests* **7**: 1-8.
- 1042 Turchin M. C., Chiang C. W., Palmer C. D., Sankararaman S., Reich D., Hirschhorn J. N., 2012
1043 Evidence of widespread selection on standing variation in Europe at height-associated
1044 SNPs. *Nature Genetics* **44**: 1015–1019.
- 1045 USDA Forest Service, *Forest Health Technology Enterprise Team*. Ft. Collins, CO.
- 1046 USDA NRCS, 2007 *Soil survey of the Tahoe Basin area, California and Nevada*.
- 1047 van Mantgem P. J., Stephenson N. L., Byrne J. C., Daniels L. D., Franklin J. F., Fulé P. Z.,
1048 Harmon M. E., Larson A. J., Smith J. M., Taylor A. H., Veblen T. T., 2009 Widespread
1049 increase of tree mortality in the western United States. *Science* **323**: 521-524.
- 1050 Vicente-Serrano S. M., Gouveia C., Camarero J. J., Beguería S., Trigo R., López-Moreno J. I.,
1051 Azorín-Molina C., Pasho E., Lorenzo-Lacruz J., Revuelto J., Morán-Tejeda E., Sanchez-
1052 Lorenzo A., 2013 Response of vegetation to drought time-scales across global land biomes.
1053 *Proceedings of the National Academy of Sciences* **110**: 52–57.
- 1054 Vizcaíno-Palomar N., Revuelta-Eugercios B., Zavala M. A., Alia R., González-Martínez S. C.,
1055 2014 The Role of Population Origin and Microenvironment in Seedling Emergence and
1056 Early Survival in Mediterranean Maritime Pine (*Pinus pinaster* Aiton) (S Delzon, Ed.). *PLoS*
1057 *ONE* **9**: e109132.
- 1058 Weir B. C., Cockerham C. C., 1984 Estimating F-statistics for the analysis of population
1059 structure. *Evolution*: 1358-1370.
- 1060 Whitlock M. C., Lotterhos K. E., 2015 Reliable detection of loci responsible for local adaptation:

- 1061 Inference of a null model through trimming the distribution of FST. *The American Naturalist*
1062 **186**: S24–S36.
- 1063 Yeaman S., 2015 Local adaptation by alleles of small effect. *The American Naturalist* **186**: S74-
1064 S89.
- 1065 Yeaman S., Whitlock M. C., 2011 The genetic architecture of adaptation under migration-
1066 selection balance. *Evolution* **65**: 1897–1911.
- 1067 Zerbino D. R., Birney E., 2008 Velvet: Algorithms for de novo short read assembly using de
1068 Bruijn graphs. *Genome Research* **18**: 821–829.
- 1069 Zhou X., Carbonetto P., Stephens M., 2013 Polygenic modeling with bayesian sparse linear
1070 mixed models. *PLoS Genetics* **9**: e1003264.
- 1071
- 1072

1073

TABLES

1074 *Table 1*

	Dick's Pass*	Freel Peak*	Heavenly	Little Round Top*	Mt. Rose Ophir*	Rifle Peak*	Snow Valley Peak*	West Shore Peaks
Population size	25 (15)	48 (19)	25 (0)	25 (14)	49 (11)	24 (15)	24 (14)	24 (0)
Ann. precipitation (mm)	1686	1019	782	1221	1186	1281	869	1585
AWC-25cm (kPa)	1.66	1.57	1.12	1.97	1.95	1.89	2.66	1.20
AWC-50cm (kPa)	2.75	2.38	2.00	2.93	2.75	3.11	4.22	2.02
CEC (cmol _c ·kg ⁻¹)	0.00	1.45	0.00	12.50	2.90	0.00	0.00	0.00
Clay (%)	6.50	4.50	6.70	14.60	3.00	6.75	6.80	6.00
Elevation (m)	2806	2865	2851	2875	2717	2819	2740	2780
GDD Aug (days)	295	190	276	211	296	235	289	279.5
GDD May (days)	0	0	6	0	11	0	2	1
Max solar rad input (%)	83.59	79.03	78.40	80.09	90.61	93.28	71.70	76.43
Max Temp – July (°C)	21.1	21.6	23.2	21.5	22.9	22.7	23.4	21.8
Min. Temp – Jan (°C)	-6.5	-8.8	-7.5	-8.0	-7.4	-7.4	-7.7	-6.6
Rock coverage (%)	31.00	18.67	25.00	14.67	7.00	30.00	26.67	42.67
Sand (%)	77.67	87.80	83.50	66.20	90.60	74.00	64.50	85.00
Silt (%)	15.8	7.7	9.7	19.1	6.4	19.2	28.7	9.0
WC-15 bar (kPa)	6.6	4.0	3.3	3.6	5.5	8.7	14.0	2.5
WC- $\frac{1}{3}$ bar (kPa)	9.7	8.0	8.4	7.3	9.8	11.4	14.4	6.2

1075 **TABLE 1** Population location and associated attributes. Population size – total (maternal trees with seedlings in common garden). Climatic values
1076 were ascertained from data spanning 1971-2000. Ann. precipitation – annual precipitation; AWC – available water capacity at 25cm or 50cm soil
1077 depth; CEC – cation exchange capacity; GDD – growing degree days above 5°C; Max solar rad input – maximum solar radiation input; WC-15bar
1078 – water capacity at -15bar (wilting point); WC- $\frac{1}{3}$ bar – water capacity at $\frac{1}{3}$ bar (field capacity). Asterisks indicates populations from which seeds
1079 sampled from cones were planted in a common garden. Environmental variables are averaged across subplots.

1080 **Table 2**

Environmental Variable	N	\overline{BF} (range)	$\overline{\rho_s}$ (range)	Median Focal $\widehat{D}_{a(ij)}$	Max. Random $\widehat{D}_{a(ij)}$	Perc. Focal < Max. Rand.
Annual Precipitation**	49	0.086–0.173	0.159–0.311	5.94e-04	1.17e-04	1.4 ($\binom{N}{2} = 1176$)
AWS0-25**	95	0.088–0.158	0.159–0.267	2.05e-04	6.84e-05	11.9 (4465)
AWS0-50**	147	0.089–0.216	0.162–0.276	1.97e-04	6.70e-05	12.6 (10731)
CEC**	14	0.086–0.152	0.228–0.345	3.75e-04	1.63e-04	8.8 (91)
Clay**	22	0.086–0.186	0.224–0.296	1.49e-04	1.27e-04	43.7 (231)
Elevation**	143	0.096–0.325	0.173–0.269	2.60e-04	8.12e-05	6.4 (10153)
GDD-Aug**	157	0.096–0.286	0.190–0.283	4.72e-04	1.13e-04	5.9 (12246)
GDD-May**	80	0.096–0.344	0.172–0.282	2.40e-04	9.60e-05	15.6 (3160)
Latitude**	119	0.091–0.193	0.161–0.246	2.00e-04	8.05e-05	15.0 (7021)
Longitude**	67	0.087–0.175	0.138–0.255	2.52e-04	9.41e-05	17.6 (2211)
Max. solar rad. Input**	144	0.090–0.361	0.246–0.318	2.33e-04	1.03e-04	21.7 (10296)
Max. Temp – July**	50	0.088–0.178	0.222–0.328	3.02e-04	8.37e-05	5.8 (1225)
Min. Temp – Jan.**	116	0.092–0.289	0.177–0.280	6.47e-04	1.28e-05	3.0 (6670)
Rock coverage**	143	0.089–0.186	0.173–0.313	3.56e-04	9.38e-05	7.6 (10153)
Sand**	111	0.090–0.206	0.167–0.254	2.11e-04	8.62e-05	18.1 (6105)
Silt**	140	0.091–0.249	0.162–0.248	2.10e-04	7.89e-05	14.0 (9730)
WC-15bar**	86	0.089–0.297	0.150–0.242	1.92e-04	8.07e-05	17.7 (3655)
WC-1/3bar**	97	0.088–0.247	0.147–0.251	2.17e-04	1.03e-05	22.7 (4656)

1081 **TABLE 2** Results from genotype-environment association with *bayenv2*. Environmental variables as in Table 1. N = number of outlier loci
1082 identified by the top 0.5% harmonic mean Bayes factor (\overline{BF}) and top 1.0% values for harmonic mean Spearman's rho ($\overline{\rho_s}$); range of \overline{BF} or $\overline{\rho_s}$ refer
1083 to minimum and maximum values from outlier loci; Median Focal $\widehat{D}_{a(ij)}$ = median $\widehat{D}_{a(ij)}$ among outlier loci; Max. Random $\widehat{D}_{a(ij)}$ = greatest value of
1084 median $\widehat{D}_{a(ij)}$ values calculated from 1000 sets of random non-outlier SNPs of equal N and similar H_E ; Perc. Focal < Max. Rand. = percentile of
1085 $\binom{N}{2}$ comparisons at which the Median Focal $\widehat{D}_{a(ij)}$ is less than Max. Random $\widehat{D}_{a(ij)}$. ** focal $\widehat{D}_{a(ij)} > 100^{\text{th}}$ percentile of random $\widehat{D}_{a(ij)}$.

1086 **Table 3**

Measure	Comparison		Mantel's <i>r</i>	<i>p</i> -value
Environment	AWS0-50	AWS0-25	0.9256	0.0020
	Clay	CEC	0.9424	0.0040
	Latitude	Elevation	0.3988	0.0490
	Longitude	Ann-ppt	0.7145	0.0030
	Max-rad-input	Latitude	0.4629	0.0370
	Sand	AWS0-50	0.4393	0.0170
	Sand	Clay	0.3723	0.0360
	Silt	AWS0-25	0.5691	0.0280
	Silt	AWS0-50	0.7552	0.0060
	Silt	Sand	0.8395	0.0010
	Tmin-Jan	GDD-Aug	0.4545	0.0470
	WC-15Bar	AWS0-25	0.6722	0.0170
	WC-15Bar	AWS0-50	0.8511	0.0030
	WC-15Bar	Silt	0.6807	0.0250
	WC-1/3bar	AWS0-25	0.6093	0.0190
	WC-1/3bar	AWS0-50	0.7761	0.0060
	WC-1/3bar	Silt	0.5582	0.0290
	WC-1/3bar	WC-15Bar	0.9423	0.0020
Phenotype	$\delta^{13}\text{C}$	$\delta^{15}\text{N}$	0.5278	0.0238
	$\delta^{15}\text{N}$	Height	0.6327	0.0198

1087 **TABLE 3** Environmental and phenotypic correlations. *Significant results from Mantel tests (9999 iterations) between pairwise environmental or*
1088 *phenotypic distance matrices calculated from centered and standardized measures. All other pairwise combinations not listed were found to have*
1089 *insignificant associations ($p > 0.05$).*

1090 **Table 4**

Selection Criterion	Phenotype	N Loci	Median Focal $\widehat{D}_{a(ij)}$	Max. Random $\widehat{D}_{a(ij)}$	Perc. Focal < Max. Rand.
$\geq 99.9^{\text{th}}$ percentile of \overline{PTP}	Bud Flush*	118	0.001398	0.001526	53.2 ($\binom{N}{2} = 6903$)
	$\delta^{13}\text{C}$	122	0.000646	0.000833	58.6 (7381)
	Height	117	0.000512	0.000609	56.4 (6786)
	$\delta^{15}\text{N}$	117	0.000583	0.000709	56.9 (6786)
	Root:Shoot**	119	0.001868	0.001720	46.6 (7021)
$\geq 99.8^{\text{th}}$ percentile of \overline{PTP}	Bud Flush*	232	0.001433	0.001568	53.7 (26796)
	$\delta^{13}\text{C}^*$	232	0.001490	0.001583	52.4 (26796)
	Height	232	0.001457	0.001650	54.9 (26796)
	$\delta^{15}\text{N}^{**}$	232	0.001566	0.001564	47.7 (26796)
	Root:Shoot**	232	0.001820	0.001610	45.3 (26796)

1091 **TABLE 4** Results from genotype-phenotype associations. Covariation among N adaptive loci identified from the top percentiles of the harmonic
1092 mean posterior inclusion probability (\overline{PTP}) estimated from GEMMA. Column names analogous to those as in Table 2. * focal $\widehat{D}_{a(ij)} > 95^{\text{th}}$ percentile
1093 of random $\widehat{D}_{a(ij)}$; ** focal $\widehat{D}_{a(ij)} > 100^{\text{th}}$ percentile of random $\widehat{D}_{a(ij)}$.

1094 **Table 5**

$pw\hat{D}_{a(ij)}$	Environmental Euclidian Distance	Mantel's r	p -value
Ann-ppt	Ann-ppt	0.7135	0.0027
GDD-May	GDD-May	0.8480	0.0013
Longitude	Longitude	0.6522	0.0024
Rock-cov	Rock-cov	0.5124	0.0145
Sand	Sand	0.5574	0.0046
Tmin-Jan	Tmin-Jan	0.5791	0.0137
WC- $\frac{1}{3}$ bar	WC- $\frac{1}{3}$ bar	0.4806	0.0361
Longitude	Ann-ppt	0.7716	0.0016
Rock-cov	Ann-ppt	0.5542	0.0221
Tmin-Jan	Ann-ppt	0.5765	0.0132
Longitude	Latitude	-0.4257	0.0347
Rock-cov	Longitude	0.5566	0.0284
Tmin-Jan	Longitude	0.4822	0.0273
Sand	Clay	0.5345	0.0232
Silt	Sand	0.4408	0.0238
WC-15bar	Tmax-July	0.3490	0.0309
WC- $\frac{1}{3}$ bar	Tmax-July	0.4539	0.0037
WC- $\frac{1}{3}$ bar	AWS0-25	0.4329	0.0384
WC- $\frac{1}{3}$ bar	AWS0-50	0.4538	0.0464
WC- $\frac{1}{3}$ bar	WC-15bar	0.5126	0.0335

1095 **TABLE 5** Signatures of allele frequency shifts associated with environmental distance. *Significant Mantel tests (9999 permutations) from*
1096 *comparisons among $pw\hat{D}_{a(ij)}$ matrices from SNPs associated with environment against environmental Euclidian distance. Above the grey line are*
1097 *significant associations among eponymous comparisons, while below the gray line are significant associations among the remaining permutations.*
1098 *Environmental variables as in Table 1.*

1099 **Table 6**

Selection criterion	$pw\widehat{D}_{a(ij)}$	Environmental Euclidian Distance	Mantel's r	p -value
99.9 th \overline{PTP}	Bud flush	GDD-Aug	0.5804	0.0181
	Bud flush	GDD-May	-0.5190	0.0458
	Bud flush	Max rad. input	-0.5486	0.0482
	Bud flush	Tmin-Jan	0.6984	0.0191
99.8 th \overline{PTP}	Bud flush	Ann-ppt	0.4309	0.0140
	Bud flush	Longitude	0.5532	0.0405
	Bud flush	Max rad. input	-0.6312	0.0127
	$\delta^{15}\text{N}$	Elevation	0.5334	0.0246
	Height	Ann-ppt	0.7210	0.0320
	$\delta^{13}\text{C}$	Ann-ppt	0.5952	0.0195

1100 **TABLE 6** Signatures of allele frequency shifts associated with environmental distance. *Significant Mantel tests (9999 permutations) from*
 1101 *comparisons among allele frequency shifts ($pw\widehat{D}_{a(ij)}$) of SNPs associated with phenotype against environmental Euclidian distance. Selection*
 1102 *Criterion refers to the process used to identify SNPs associated with phenotype.*

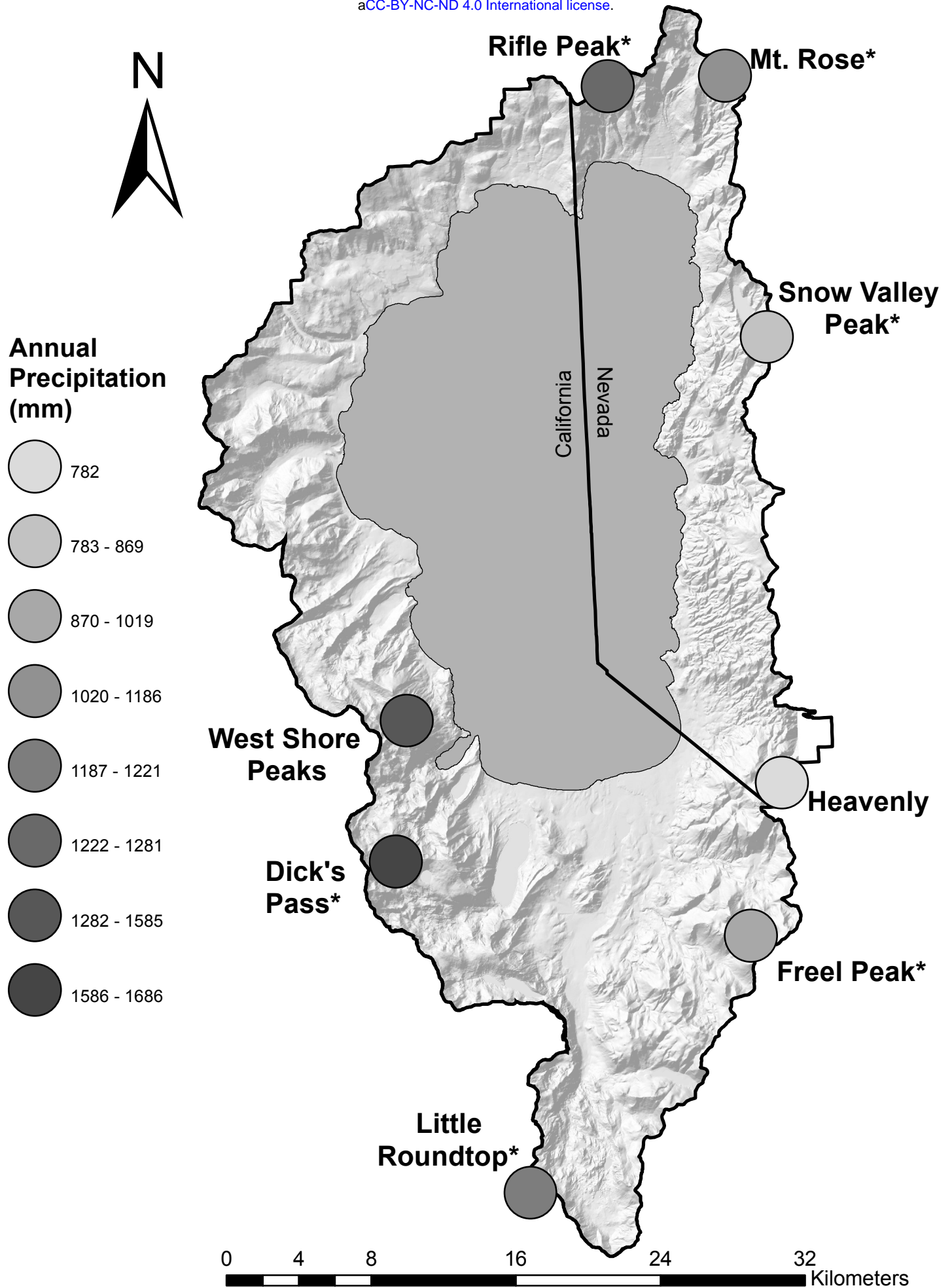
1103

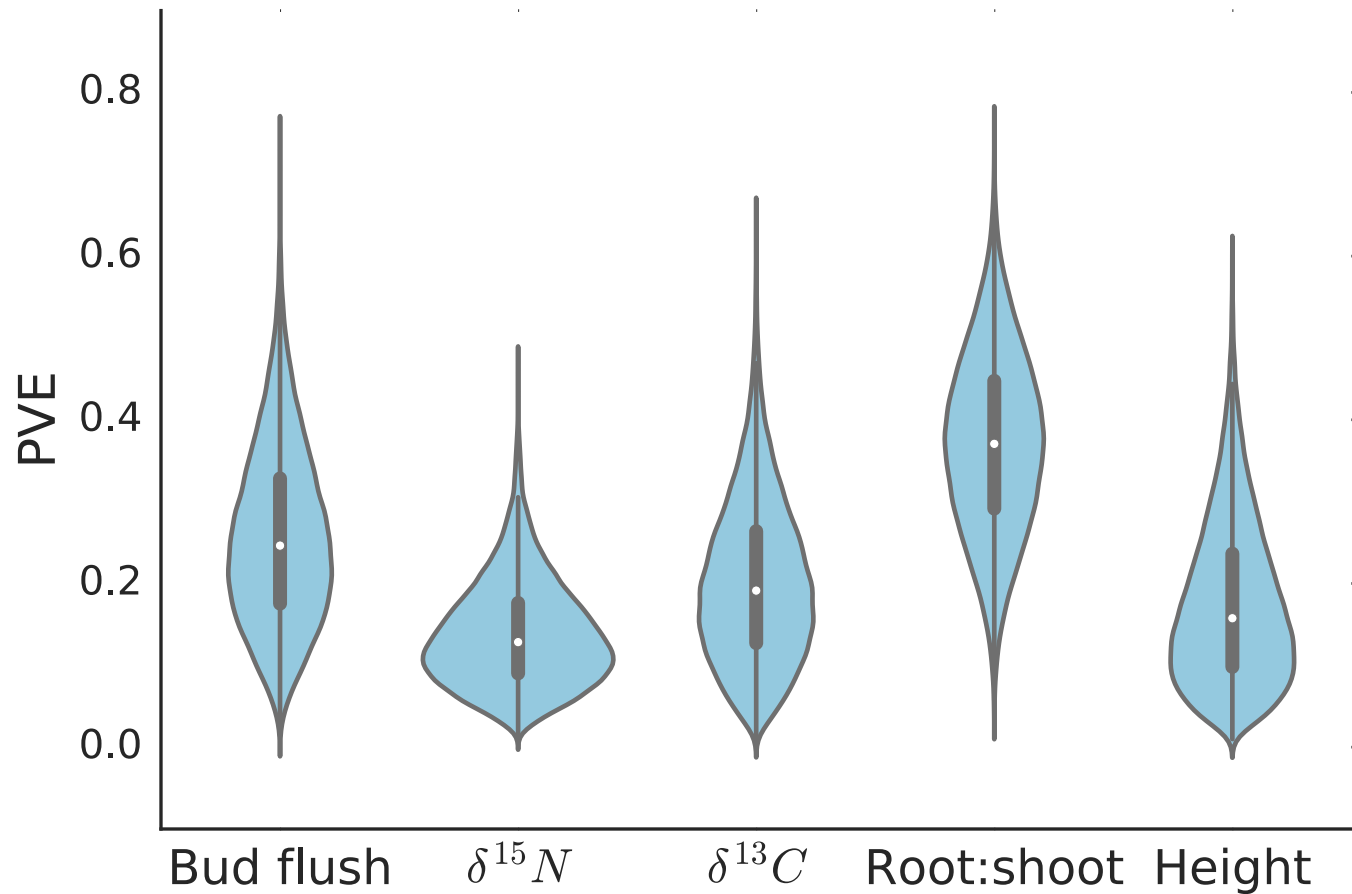
FIGURE LEGENDS

1104 **Figure 1** Populations used for sampling *P. albicaulis* within the Lake Tahoe Basin (dark outline). Annual
1105 precipitation is given for each population to demonstrate the west-east rain shadow experienced across
1106 short spatial scales. Asterisks indicate populations in the common garden study.

1107

1108 **Figure 2** Violin plots for the kernel density estimator of the posterior distributions (blue) taken from GEMMA
1109 for (A) the proportion of variance explained by SNPs included in the model (PVE) and (B) the number of
1110 SNPs underlying the phenotypic trait (N_{SNP}). Priors for N_{SNP} and PVE were [1,300] and [0.01,0.9],
1111 respectively. Grey vertical bars display the first through third interquartile range with the median
1112 represented by the white dot.



A

B